or both. (1) The ~740–750-cm$^{-1}$ "$\nu_{15}$" RR band (maximized with $Q_y$ excitation) is sensitive to both pyrroline stereochemistry and to macrocyclic conformation: the *frequency* observed for *trans*-M(OEC) is greater than that of *cis*-M(OEC), whereas the *intensity* observed is greater for $S_4$-ruffled Ni(OEC) than for planar Cu(OEC). (2) The frequencies of bands in the ~1150–1220-cm$^{-1}$ IR spectra are sensitive to pyrroline stereochemistry: the $C_b$–H deformation modes of *cis*-M(OEC) are higher in frequency than those of *trans*-M(OEC). (3) Extension of the core size/RR frequency inverse correlation of metalloporphyrins to the -chlorins indicates sensitivity to both stereochemistry and macrocyclic conformation: RR frequencies of *cis*-M(OEC) are higher than those of *trans*-M(OEC); thus, *cis*-M(OEC) complexes have a smaller core size than *trans*-M(OEC). Similarly, RR frequencies of *cis*- and *trans*-Ni(OEC) are higher than those of the Cu(OEC) complexes; thus, $S_4$-ruffled Ni(OEC) complexes have a smaller core size than planar Cu(OEC) complexes. (4) The electronic absorption spectra of M(OEC) are also sensitive both to the stereochemistry at the pyrroline ring and to the macrocyclic conformation: the $Q_y$ transitions of *cis*-M(OEC) are red-shifted from those of *trans*-M(OEC), whereas the Soret/$Q_y$ intensity ratio of the planar Cu(OEC) complexes is greater than that of the ruffled Ni(OEC) complexes.

Thus, "local" structural modifications have a significant effect on both the vibrational modes of chlorins and their electronic absorption properties. Consequently, the influences of nonconjugated substituents and their conformation and stereochemistry, as well as the overall macrocyclic conformation of chlorins and other hydroporphyrins, should be considered in the analysis of their spectral properties.

**Acknowledgment** is made to the donors of the Petroleum Research Fund (L.A.A.), administered by the American Chemical Society, for partial support of this research. This work was also supported by the National Institutes of Health (Grant GM 34468 to T.M.L. and L.A.A. and Grant GM 33882 to A.M.S.) and by the Camille and Henry Dreyfus Foundation (Distinguished New Faculty Award to A.M.S.). We thank Professor James Kincaid for sharing unpublished data and Ron Shigeta for technical assistance.

---

Contribution from the Department of Chemistry, University of North Carolina, Chapel Hill, North Carolina 27514

# Synthetic Control of Excited-State Properties in Ligand-Bridged Complexes of Rhenium(I). Intramolecular Energy Transfer by an Electron-Transfer/Energy-Transfer Cascade

Gilles Tapolsky, Rich Duesing, and Thomas J. Meyer*

*Received August 15, 1989*

In the series of complexes $[(4,4'\text{-}(X)_2\text{-}2,2'\text{-bpy})(CO)_3Re^I(4,4'\text{-bpy})Re^I(CO)_3(4,4'\text{-}(Y)_2\text{-}2,2'\text{-bpy})]^{2+}$ (X, Y = H, $CH_3$, $NH_2$, $CO_2Et$), the ultimate site of the excited electron following metal-to-ligand charge-transfer (MLCT) excitation has been studied by transient absorbance and emission spectroscopies in polar organic solvents. The electron-donating groups $NH_2$ and Me increase the energy of the $\pi^*$ levels of the 2,2'-bpy ligand. They lead to localization of the excited electron on the bridging 4,4'-bpy ligand, as shown by the appearance of an absorption feature at 570–610 nm in $CH_3CN$ in transient absorbance difference spectra. Electron-withdrawing $CO_2Et$ groups lower the energy of the $\pi^*$ levels and lead to localization of the excited electron on the 2,2'-bpy ligand, as shown by the appearance of a narrow transient absorption feature at 380–385 nm in $CH_3CN$. With X = Y = H, a solvent-dependent equilibrium exists between the 2,2'-bpy and 4,4'-bpy states. In the asymmetrical complexes with X = $NH_2$ or H and Y = $CO_2Et$, rapid ($k > 2 \times 10^8$ s$^{-1}$) intramolecular energy transfer occurs following Re → 4,4'-$(X)_2$-bpy MLCT excitation in $CH_3CN$. Intramolecular energy transfer continues to occur in a 4:1 (v/v) ethanol/methanol glass at 77 K. With 3,3'-$(Me)_2$-4,4'-bpy as the bridging ligand, the rate constant for energy transfer is far slower ($k < 4 \times 10^6$ s$^{-1}$), suggesting that energy transfer in the 4,4'-bpy bridged complex may occur by an electron-transfer/energy-transfer pathway.

## Introduction

Ligand-bridged metal complexes have provided a useful basis for theoretical and experimental studies on light-induced intramolecular electron and energy transfer.[1,2] For example, in mixed valence complexes such as $[(NH_3)_5Ru^{II}(L)Ru^{III}(NH_3)_5]^{5+}$ or $[(bpy)_2ClRu^{II}(L)Ru^{III}Cl(bpy)_2]^{3+}$ (L is 4,4'-bipyridine (4,4'-bpy) or pyrazine (pz); bpy is 2,2'-bipyridine), the existence of light-induced electron transfer is evidenced by the appearance of intervalence transfer absorption bands.[3,4] In complexes such as $[(NH_3)_5Ru^{II}(pz)Ru^{III}(edta)]$[5] or $[(bpy)_2(CO)Os^{II}(4,4'\text{-bpy})Os^{II}(phen)(dppe)(Cl)]^{3+}$ (phen is 1,10-phenanthroline, dppe is *cis*-$Ph_2PCH{=}CHPPh_2$),[6] metal-to-ligand charge-transfer (MLCT) excitation is followed by electron transfer across the ligand bridge.[7,8]

(1) (a) Woiteller, S.; Launay, J. P.; Joachim, C. *Chem. Phys.* **1989**, *131*, 481. (b) Mikkelsen, K. V.; Ratner, M. A. *J. Phys. Chem.* **1989**, *93*, 1759. (c) Kuznets, A. M.; Ultstrup, J. *J. Chem. Phys.* **1981**, *75*, 2047. (d) Uzer, T.; Hynes, J. T. *J. Phys. Chem.* **1986**, *90*, 3524. (e) Schipper, P. E. *J. Phys. Chem.* **1986**, *90*, 2351. (f) Piepho, S. B.; Krausz, E. R.; Schatz, P. N. *J. Am. Chem. Soc.* **1978**, *100*, 2996. (g) Wong, K. Y.; Schatz, P. N.; Piepho, S. B. *J. Am. Chem. Soc.* **1979**, *101*, 2793.

(2) (a) Wacholtz, W. F.; Auerbach, R. A.; Schmehl, R. S. *Inorg. Chem.* **1986**, *25*, 227. (b) Balzani, V.; Barigelletti, F.; Campagna, S.; Belser, P.; von Zelewsky, A. *Coord. Chem. Rev.* **1988**, *84*, 85. (c) Murphy, W. R., Jr.; Brewer, K. T.; Petersen, J. D. *Inorg. Chem.* **1987**, *26*, 3376. (d) Fuchs, Y.; Lofters, S.; Dieter, T.; Shi, W.; Morgan, R.; Strekas, T. C.; Gafney, H. D.; Baker, A. D. *J. Am. Chem. Soc.* **1987**, *109*, 2691. (e) Nishizawa, M.; Ford, P. C. *Inorg. Chem.* **1981**, *20*, 2016. (f) Ruminski, R. R.; Cockroft, T.; Shoup, M. *Inorg. Chem.* **1988**, *27*, 4026. (g) Braunstein, H. C.; Baker, D. A.; Strekas, T. C.; Gafney, D. H. *Inorg. Chem.* **1984**, *23*, 857. (h) Ruminski, R. R.; Kiplinger, J.; Cockroft, T.; Chase, C. *Inorg. Chem.* **1989**, *28*, 370. (i) Curtis, J. C.; Bernstein, J. S.; Meyer, T. J. *Inorg. Chem.* **1985**, *24*, 385.

(3) (a) Creutz, C.; Taube, H. *J. Am. Chem. Soc.* **1969**, *91*, 3988. (b) Fischer, H.; Tom, G.; Taube, H. *J. Am. Chem. Soc.* **1976**, *98*, 5512. (c) Powers, M. J.; Meyer, T. J. *J. Am. Chem. Soc.* **1980**, *102*, 1289. (d) Hupp, J. T.; Meyer, T. J. *Inorg. Chem.* **1987**, *26*, 2332. (e) Richardson, D. E.; Taube, H. *J. Am. Chem. Soc.* **1983**, *105*, 40. (f) Lavallee, D. K.; Fleischer, E. B. *J. Am. Chem. Soc.* **1972**, *94*, 2583.

(4) (a) Hush, N. S. *Prog. Inorg. Chem.* **1967**, *8*, 391. (b) Creutz, C. *Prog. Inorg. Chem.* **1983**, *30*, 1.

(5) Creutz, C.; Kroger, P.; Matsubara, T.; Netzel, T.; Sutin, N. *J. Am. Chem. Soc.* **1979**, *101*, 5442.

(6) Schanze, K. S.; Neyhart, G. A.; Meyer, T. J. *J. Phys. Chem.* **1986**, *90*, 2182.

(7) (a) Kambara, T.; Hendrickson, D. N.; Sorai, M.; Oh, S. M. *J. Chem. Phys.* **1986**, *85*, 2895. (b) Oh, S. M.; Hendrickson, D. N.; Hassett, K. L.; Davis, R. E. *J. Am. Chem. Soc.* **1985**, *107*, 8009. (c) Dong, T.-Y.; Kambara, T.; Hendrickson, D. N. *J. Am. Chem. Soc.* **1986**, *108*, 4423. (d) Dong, T.-Y.; Hendrickson, D. N.; Iwai, K.; Cohn, M. J.; Geib, S. J.; Rheingold, A. L.; Sano, H.; Motoyama, I.; Nakashima, S. *J. Am. Chem. Soc.* **1985**, *107*, 7996. (e) Woehler, S. E.; Wittebort, R. J.; Oh, S. M.; Hendrickson, D. N.; Inniss, D.; Strouse, C. E. *J. Am. Chem. Soc.* **1986**, *108*, 2938. (f) Dong, T.-Y.; Hendrickson, D. N.; Pierpont, C. G.; Moore, M. F. *J. Am. Chem. Soc.* **1986**, *108*, 963.

0020-1669/90/1329-2285$02.50/0 

In earlier work, Wrighton and co-workers introduced the complex $[(bpy)Re^{I}(CO)_3Cl]$ and its derivatives as MLCT emitters.[9] From the synthetic point of view, the $Re^{I}$-based complexes offer several advantages. These include the ease of exchange of $Cl^-$ for other ligands and the ability to incorporate modified bpy ligands.[10] We have utilized this synthetic chemistry to prepare ligand-bridged complexes of $Re^{I}$ such as $[(bpy)(CO)_3Re^{I}(4,4'\text{-}bpy)Re^{I}(CO)_3(bpy)]^{2+}$ in order to explore two issues. One was to utilize the substituent effects at bpy to create an electronic basis for the localization of the excited electron either at 2,2'-bpy or at the 4,4'-bpy bridging ligand. The second goal was to utilize asymmetrical complexes, where the asymmetry is induced by changes in ligand substituents at 2,2'-bpy in order to study intramolecular energy transfer across the ligand bridge. Part of this work has appeared in a preliminary communication.[11] The structures and abbreviations of the ligands used in this study are illustrated as follows:

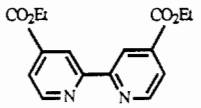

$(b(CO_2Et)_2)$

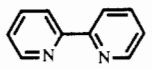

(b or bpy)

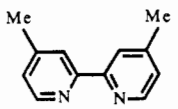

$(b(Me)_2)$

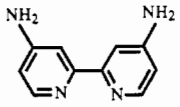

$(b(NH_2)_2)$

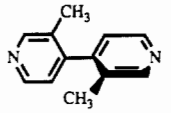

(3,3'-$(CH_3)_2$-4,4'-bpy)

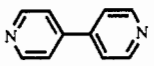

(4,4'-bpy)

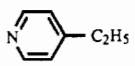

(4-Etpy)

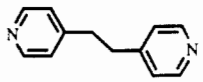

(bpa)

## Experimental Section

**Materials, Methods, and Instrumentation.** UV–vis spectra were recorded on a Hewlett-Packard 8451A diode-array spectrophotometer in 1 cm path length cuvettes. $^1H$ NMR spectra were recorded in $CD_3CN$ on a Brucker 200- or 300-MHz spectrometer. Emission spectra were recorded on a Spex Fluorolog-F212 emission spectrometer equipped with a 450-W xenon lamp and a cooled Hamamatsu R928 photomultiplier tube (PMT) and were corrected for instrument response. Cyclic voltammograms were recorded by using a Princeton Applied Research Model 173 potentiostat, a Princeton Applied Research Model 175 sweep generator, and a Soltec Model 6414S XY recorder. They were obtained in argon-deaerated 0.1 M $[N(n\text{-}C_4H_9)_4](PF_6)/CH_3CN$ solutions vs SSCE by using a platinum disk as the working electrode at scan rates of 0.1 V/s. The supporting electrolyte was recrystallized twice from $CH_3CN/H_2O$. Emission lifetime measurements were obtained by using a PRA LN 1000/LN 102 nitrogen laser/dye laser combination for sample excitation. Emission was monitored at a right angle to the excitation by using a PRA B204-3 monochromator and a cooled, 10-stage, Hamamatsu R928 PMT coupled to either a LeCroy 9400 or a LeCroy 8013 digital oscilloscope interfaced to an IBM PC. The absorbance (in 1-cm cuvettes) of the various solutions was ~0.1 at the excitation wavelength. Solutions were deoxygenated by Ar bubbling.

Transient absorbance measurements were performed by using the third harmonic of a Quanta Ray DCR-2A Nd:YAG laser. The excitation beam was at a right angle to an Applied Photophysics laser kinetic spectrometer including a 250-W pulsed Xe arc probe source, a $f/3.4$ grating monochromator, and a 5-stage PMT. The output was coupled to a Tektronix 7912 digital oscilloscope interfaced to an IBM PC. Electronic control and synchronization of laser, probe, and digital oscilloscope were achieved by electronics of our own design. Solutions were freeze–pump–thaw deoxygenated for at least four cycles before use. The ground-state absorbance at the excitation wavelength was typically ~0.7. For reasons unknown to us, the complexes $[(b(Me)_2)(CO)_3Re^{I}(4,4'\text{-}bpy)Re^{I}(CO)_3(b(Me)_2)]^{2+}$ and $[(b(Me)_2)(CO)_3Re^{I}(4,4'\text{-}bpy)Re^{I}(CO)_3(b)]^{2+}$ underwent noticeable photochemical degradation during the transient absorbance experiments. This was not a problem for the other complexes characterized in the study.

Intensity–time-decay curves from the transient emission or absorbance experiments were fit to the single-exponential or biexponential functions in eq 1 or 2 by using a Levenberg–Marquadt fitting routine.[13]

$$A(t) \text{ or } I(t) = a_1 \exp[-(k_1 t)] + c \quad (1)$$

$$A(t) \text{ or } I(t) = a_1 \exp[-(k_1 t)] + a_2 \exp[-(k_2 t)] \quad (2)$$

Solvents were used without purification unless otherwise specified. Acetonitrile, propylene carbonate, and methanol were spectrophotometric grade (Burdick & Jackson). The solvents 1,2-dichloroethane, and dimethyl sulfoxide (DMSO) were spectrophotometric grade and were obtained from Aldrich. Ethyl ether and 2-MeTHF were reagent grade and were purchased from Fisher Scientific and distilled over potassium. Chemical analyses were performed by Galbraith Laboratories (Knoxville, TN).

2,2'-Bipyridine, 4,4'-bipyridine, and the salts $[N(n\text{-}C_4H_9)_4](PF_6)$ and $[NH_4](PF_6)$ were obtained from Aldrich. The bipyridyl compounds were recrystallized from acetonitrile/ether and the salts from ethanol. $Re(CO)_5Cl$ was purchased from Pressure Chemical Co. 4,4'-$(NH_2)_2$-bpy, 4,4'-$(CO_2Et)_2$-bpy, and $[(4,4'\text{-}(X)_2\text{-}bpy)(CO)_3Re^{I}(CF_3SO_3)]$ were prepared according to literature procedures.[12]

**Syntheses. $[(4,4'\text{-}(Me)_2\text{-}bpy)(CO)_3Re^{I}(4,4'\text{-}bpy)](PF_6)$.** To 300 mg (0.5 mmol) of $[(4,4'\text{-}(Me)_2\text{-}bpy)(CO)_3Re^{I}(TFMS)]$ in 25 mL of THF was added 700 mg (4.5 mmol) of 4,4'-bipyridine. The solution, protected from the light and under an Ar blanket, was heated for 3 h at reflux. After the solution was cooled to room temperature, ether was slowly added to the filtered solution to give a yellow precipitate. It was collected, washed, dried under vacuum, and then redissolved in acetone. This solution was added to an aqueous solution of $[NH_4](PF_6)$. The resulting $PF_6^-$ salt was collected, washed with water, and dried under vacuum. It was then chromatographed on silica gel (75/230 mesh) with 1:4 (v/v) acetonitrile/methylene chloride as eluent. The yellow eluted fraction was evaporated to dryness. The solid material was redissolved in acetone and reprecipitated by addition of ether to give a yellow solid, 95 mg (0.12 mol), 24%. Anal. Calcd for $C_{25}H_{20}N_4O_3RePF_6$: C, 39.42; H, 2.63; N, 7.36. Found: C, 38.50; H, 2.84; N, 6.86. $^1H$ NMR, ppm vs TMS (integration; multiplicity, coupling; assignment): 9.05 (2 H; d, 5.4 Hz; 6,6' of $b(X)_2$; 8.7 (2 H; d, 5.6 Hz; 2,6 of 4,4'-bpy); 8.34 (2 H; d, 6.7 Hz; 2',6' of 4,4'-bpy); 8.23 (2 H; s; 3,3' of $b(X)_2$); 7.6 (6 H; m; 5,5' of $b(X)_2$ and 3,3',5,5' of 4,4'-bpy); 2.54 (6 H; s; $CH_3$).

**$[(bpy)(CO)_3Re^{I}(4,4'\text{-}bpy)](PF_6)$.** The solid $[(bpy)(CO)_3Re^{I}(TFMS)]$, 1.2 g (2.1 mmol), was dissolved in 60 mL of a 2:1 (v/v) $EtOH/H_2O$ mixture heated at reflux. Solid 4,4'-bipyridine, 500 mg (3.2 mmol), was added, and the solution was heated at reflux for an additional 6 h. After the 4,4'-bpy solution was cooled to room temperature, a saturated aqueous solution of $[NH_4](PF_6)$ was added. The mixture was concen-

(8) (a) Furue, M.; Kinoshita, S.; Kushida, T. *Chem. Phys. Lett.* **1987**, 2355. (b) Gelroth, J. A.; Figard, J. E.; Petersen, J. D. *J. Am. Chem. Soc.* **1979**, *101*, 3649. (c) Schmehl, R. H.; Auerbach, R. A.; Wacholtz, W. F. *J. Phys. Chem.* **1988**, *92*, 6202. (d) Moore, K. J.; Lee, L.; Figard, J. E.; Gelroth, A.; Wohlers, D. H.; Petersen, J. D. *J. Am. Chem. Soc.* **1983**, *105*, 2274. (e) Petersen, J. D.; Murphy, W. R., Jr.; Sahai, R.; Brewer, K. T.; Ruminski, R. R. *Coord. Chem. Rev.* **1985**, *64*, 261.

(9) (a) Wrighton, M. S.; Morse, D. L. *J. Organomet. Chem.* **1975**, *97*, 405. (b) Morse, D. L.; Wrighton, M. *J. Am. Chem. Soc.* **1974**, *96*, 998. (c) Luong, J. C.; Nadjo, L.; Wrighton, M. S. *J. Am. Chem. Soc.* **1978**, *100*, 5790. (d) Kalyanasundaran, K. *J. Chem. Soc., Faraday Trans. 2* **1986**, *82*, 2401. (e) Juris, A.; Campagna, S.; Ibied, I.; Lehn, J.-M.; Ziessel, R. *Inorg. Chem.* **1988**, *27*, 4007.

(10) (a) Juris, A.; Campagna, S.; Balzani, V.; Gremaud, G.; von Zelewsky, A. *Inorg. Chem.* **1988**, *27*, 3652. (b) Hosek, W.; Tysoe, W. A.; Gafney, H. D.; Baker, D. A.; Strekas, T. C. *Inorg. Chem.* **1989**, *28*, 1228. (c) Della Ciana, L.; Hamachi, I.; Meyer, T. J. *J. Org. Chem.* **1989**, *54*, 1731.

(11) Tapolsky, G.; Duesing, R.; Meyer, T. J. *J. Phys. Chem.* **1989**, *93*, 3885.

(12) (a) Sullivan, B. P.; Meyer, T. J. *J. Chem. Soc., Chem. Commun.* **1984**, 1244. (b) Sullivan, B. P.; Silliman, S.; Thorpe, H.; Meyer, T. J. *Inorg. Chem.*, in press. (c) Della Ciana, L.; Dressik, W.; Worl, L.; Meyer, T. J. Manuscript in preparation.

(13) Seber, G. A.; Wild, C. J. *Non Linear Regression*; Wiley: New York, 1987.

trated via rotary evaporation to one-third of the original volume to give a yellow precipitate. The precipitate was collected and washed with water, ethanol, and ether. It was redissolved in acetone (10 mL) and ether (7 × 10 mL) was slowely added to give a yellow crystalline product, which was collected, washed, and dried under vacuum to give 1.57 mmol of a yellow solid. The yield was 65%. $^1$H NMR, ppm: 9.2 (2 H; d, 5.5 Hz; 6,6′ of b); 8.6–8.4 (6 H; m, 3,3′ of b and 2,6 and 2′,6′ of 4,4′-bpy); 7.9 (2 H; d of d, 5.5 and 1.2 Hz; 4,4′ of b); 7.75 (4 H; d of d, 5.5 and 1.5 Hz; 5,5′ of b); 7.45 (4 H; d of d, 5.2 and 1.5 Hz; 3,3′ and 6,6′ of 4,4′-bpy).

**[(4,4′-$(CO_2Et)_2$-bpy)$(CO)_3Re^I$(4,4′-bpy)]$(PF_6)$.** Solid 4,4′-bipyridine, 780 mg (5 mmol), and 900 mg (1.25 mmol) of [(4,4′-$(CO_2Et)_2$-bpy)-$(CO)_3Re^I$(TFMS)] were dissolved in 35 mL of THF. The solution was heated at reflux for 6 h. After the 4,4′-bpy solution was cooled to room temperature, a saturated aqueous solution of $[NH_4](PF_6)$ was added and the resulting slurry was evaporated to dryness by rotary evaporation. The product was chromatographed on silica gel (75–230 mesh) initially with 1:2 (v/v) $CH_3CN/CH_2Cl_2$ and finally with 1:10 (v/v) acetone/water 0.05 M in $[NH_4](PF_6)$. The eluent was evaporated, the resulting solid was dissolved in acetone, and the final product was reprecipitated by adding this solution to an ether solution to give 756 mg (0.87 mmol) of an orange solid. The yield was 73%. $^1$H NMR, ppm: 9.41 (2 H; d of d, 5.7 and 0.5 Hz; 6,6′ of b$(X)_2$); 8.89 (2 H; d of d, 1 and 0.6 Hz; 3,3′ of b$(X)_2$); 8.66 (2 H; d of d, 4.5 and 1.7 Hz; 2,6 of 4,4′-bpy); 8.30 (2 H; d of d, 5.2 and 1.6 Hz; 2′,6′ of 4,4′-bpy); 8.21 (2 H; d of d, 5.6 and 1.3 Hz; 5,5′ of b$(X)_2$); 7.56 (2 H; d of d, 5.2 and 1.6 Hz; 3′,5′ of 4,4′-bpy); 7.50 (2 H; d of d, 4.5 and 1.6 Hz; 3,5 of 4,4′-bpy); 4.46 (4 H; q, 7.1 Hz; $OCH_2CH_3$); 1.42 (12 H; t, 7.1 Hz; $OCH_2CH_3$).

**[(bpy)$(CO)_3Re^I$(bpa)$Re^I(CO)_3$(bpy)]$(PF_6)_2$.** To 570 mg (~1 mmol) of [bpy$(CO)_3Re^I(CF_3SO_3)$] in refluxing THF (30 mL) was added 40 mg (~0.25 mmol) of 4,4′-bipyridine. The yellow solution was heated at reflux for 4 h while protected from light and under an Ar blanket. During the reaction, a yellow precipitate of the $CF_3SO_3^-$ salt appeared. The warm solution was filtered and the yellow solid that was collected was washed with ether and dried under vacuum. It was purified by dissolving in acetone and reprecipitating by addition to a saturated aqueous solution of $[NH_4](PF_6)$. The yellow precipitate was collected, washed with water, ethanol, and ether, and dried under vacuum. It was chromatographed on silica gel (70–230 mesh) by using a 1:2 (v/v) $CH_3CN/CH_2Cl_2$ solvent mixture. The product was dried, redissolved in $CH_3CN$, and precipitated by the addition of ether. Dried under vacuum, 249 mg (0.18 mmol) of product was obtained. The yield was 75% based on 4,4′-bipyridine as the limiting reagent. Anal. Calcd for $C_{38}H_{28}N_6O_6Re_2P_2F_{12}$: C, 34.39; H, 2.11; N, 6.33. Found: C, 33.2; H, 2.10; N, 6.44. $^1$H NMR, ppm: 9.18 (4 H; d; 5 Hz; 6,6′ of b); 8.35 (4 H; d; 7 Hz; 3,3′ of b); 8.25 (4 H; d of d, 1.5 and 7.5 Hz; 4,4′ of b); 8.06 (4 H; d of d, 5.3 and 1.5 Hz; 2,2′ and 6,6′ of pyridyl); 7.76 (4 H; d of d, 1.5 and 5.5 Hz; 5,5′ of b); 7.07 (4 H; d of d, 5.2 and 1.5 Hz; 3,3′ and 5,5′ of pyridyl); 2.72 (4 H; s; $CH_2$).

**[(4,4′-$(NH_2)_2$-bpy)$(CO)_3Re^I$(4,4′-bpy)$Re^I(CO)_3$(4,4′-$(NH_2)_2$-bpy)]-$(PF_6)_2$.** To 40 mg (~0.25 mmol) of 4,4′-bipyridine dissolved in 25 mL of THF was added 360 mg (~0.6 mmol) of [(4,4′-$(NH_2)_2$-bpy)-$(CO)_3Re^I$(TFMS)]. The solution was heated gently at reflux for about 6 h. A yellow precipitate appeared after ~2 h of heating at reflux. The solution was allowed to cool to room temperature and filtered, and the yellow precipitate was collected, washed with cold THF, and dried under vacuum overnight. The solid material became an oil after drying. The oil was dissolved in acetone, and a yellow solid was precipitated by pouring into an aqueous solution of $[NH_4](PF_6)$. The yellow precipitate was washed with water, cold ethanol, and ether and dried under vacuum, giving 300 mg (0.22 mmol) of a yellow solid. The yield was 88% based on 4,4′-bpy. The compound was recrystallized from either THF or MeOH. Anal. Calcd for $C_{36}H_{28}N_{10}O_6Re_2P_2F_{12}$: C, 31.81; H, 2.06; N, 10.31; P, 4.56. Found: C, 31.55; H, 2.49; N, 9.37; P, 4.29. $^1$H NMR, ppm: 8.49 (4 H; d, 6.49 Hz; 6,6′ of b$(X)_2$); 8.33 (4 H; d of d, 5.3 and 1.6 Hz; 2,2′ and 6,6′ of 4,4′-bpy); 7.52 (4 H; d of d, 5.3 and 1.6 Hz; 3,3′ and 5,5′ of 4,4′-bpy); 7.18 (4 H; d, 2.5 Hz; 3,3′ of b$(X)_2$); 6.76 (4 H; d of d, 6.4 and 2.5 Hz; 5,5′ of b$(X)_2$); 5.84 (8 H; s; $NH_2$).

**[(4,4′-$(Me)_2$-bpy)$(CO)_3Re^I$(4,4′-bpy)$Re^I(CO)_3$(4,4′-$(Me)_2$-bpy)]-$(PF_6)_2$.** This salt was synthesized by following the procedure used for the previous complex. It was recrystallized by slow evaporation from a 1:1 (v/v) acetone/chloroform mixture to give 120 mg (0.09 mol); the yield was 45% based on 4,4′-bpy. Anal. Calcd for $C_{40}H_{32}N_6O_6Re_2P_2F_{12}$: C, 35.45; H, 2.36; N, 6.20; P, 4.58. Found: C, 35.56; H, 2.57; N, 5.86; P, 5.68. $^1$H NMR, ppm: 9.02 (4 H; d, 5.1 Hz; 6,6′ of b$(X)_2$); 8.8 (4 H; d of d, 5.3 and 1.4 Hz; 2,2′ and 6,6′ of 4,4′-bpy); 8.21 (4 H; s; 3,3′ of b$(X)_2$); 7.58 (4 H; d of d, 5.1 and 1.6 Hz; 5,5′ of b$(X)_2$; 7.45 (4 H; d of d, 5.3 and 1.4 Hz; 3,3′ and 5,5′ of 4,4′-bpy); 2.54 (6 H; s; $CH_3$).

**[(bpy)$(CO_3)Re^I$(4,4′-bpy)$Re^I(CO_3)$(bpy)]$(PF_6)_2$.** The same procedure was utilized as for the previous complex. The yield was 77%, 402 mg (0.31 mmol). Anal. Calcd for $C_{36}H_{24}N_6O_6Re_2P_2F_{12}$: C, 33.28; H, 1.85; N, 6.47; P, 4.78. Found: C, 33.20; H, 1.63; N, 6.24; P, 5.28. $^1$H NMR, ppm: 9.2 (4 H; d, 5.5 Hz; 6,6′ of b); 8.4–8.15 (12 H, d; 3,3′ of b and 2,6 and 2′,6′ of 4,4′-bpy, then 4,4′ of b); 7.75 (4 H; d of d, 5.5 and 1.5 Hz; 5,5′ of b); 7.43 (4 H; d of d, 5.2 and 1.5 Hz; 3,3′ and 6,6′ of 4,4′-bpy).

**[(4,4′-$(CO_2Et)_2$-bpy)$(CO_3)Re^I$(4,4′-bpy)$Re^I(CO_3)$(4,4′-$(CO_2Et)_2$-bpy)]$(CF_3SO_3)_2$.** A quantity of 0.7 mmol of [(4,4′-$(CO_2Et)_2$-bpy)-$(CO_3)Re^I$(TFMS)] and 0.3 mmol of 4,4′-bpy in 15 mL of THF were gently heated at reflux overnight. An orange product precipitated spontaneously. The warm solution was filtered and the precipitate washed with cold THF and ether. After drying under vacuum overnight, the solid material was dissolved in acetonitrile, reprecipitated with ether, washed with ether, and dried under vacuum to give 287 mg (0.18 mmol) of an orange solid. The yield based on 4,4′-bpy was 60%. Anal. Calcd for $C_{50}H_{40}N_6Re_2S_2F_6$: C, 37.64; H, 2.51; N, 5.27. Found: C, 36.67; H, 2.66; N, 5.05. $^1$H NMR, ppm: 9.41 (4 H; d of d, 5.7 and 0.5 Hz; 6,6′ of b$(X)_2$); 8.86 (4 H; d, 0.5 Hz; 3,3′ of b$(X)_2$); 8.26 (4 H; d of d, 6.7 and 1.7 Hz; 2,2′ and 6,6′ of 4,4′-bpy); 8.2 (4 H; d, 5.7 Hz; 5,5′ of b$(X)_2$); 7.42 (4 H; d of d, 6.7 and 1.8 Hz; 3,3′ and 5,5′ of 4,4′-bpy); 4.46 (8 H, q, 7.1 Hz; $OCH_2CH_3$); 1.42 (12 H; t, 7.1 Hz; $OCH_2CH_3$).

**[(4,4′-$(NH_2)_2$-bpy)$(CO)_3Re^I$(4,4′-bpy)$Re^I(CO)_3$(bpy)]$(PF_6)_2$.** A quantity of 310 mg (0.5 mmol) of [(4,4′-$(NH_2)_2$-bpy)$(CO)_3Re^I$(TFMS)] in 10 mL of THF was added to 290 mg (0.39 mmol) of [(bpy)-$(CO)_3Re^I$(4,4′-bpy)]$(PF_6)$ in 5 mL of acetone. The resulting solution was heated at reflux for 3 h. After cooling to room temperature, the solution was filtered, and 50 mL of ether was slowly added to the filtrate. The yellow precipitate was collected, washed with ether, and dried under vacuum. The solid material was dissolved in acetone, the solution filtered and added to an aqueous solution of $[NH_4](PF_6)$. The resulting yellow precipitate was collected, dried, and chromatographed on silica gel (75–230 mesh) by using a 1:3 (v/v) acetonitrile/methylene chloride mixture as eluent. The product was dried, redissolved in acetonitrile, and reprecipitated by addition to ether. The product was recrystallized by slow evporation in 1:1 (v/v) acetone/methanol to give 440 mg (0.33 mmol) of a yellow solid. The yield was 87% based on [(bpy)-$(CO)_3Re^I$(4,4′-bpy)]$(PF_6)$. Anal. Calcd for $C_{36}H_{26}N_8O_6Re_2P_2F_{12}$: C, 32.53; H, 1.96; N, 8.43; P, 4.67. Found: C, 32.56; H, 2.36; N, 8.71; P, 4.24. $^1$H NMR, ppm: 9.2 (2 H; d of d; 6,6′ of b); 8.55 (2 H; d, 6.4 Hz; 6,6′ of b$(NH_2)_2$); 8.3 (8 H; m; 3,3′ and 4,4′ of b and 2,2′ and 6,6′ of 4,4′-bpy); 7.78 (2 H; d of d; 5,5′ of b); 7.5 (4 H; d of d; 3,3′ and 5,5′ of 4,4′-bpy); 7.18 (2 H; d, 2.5 Hz; 3,3′ of b$(NH_2)_2$); 6.75 (2 H; d of d, 6.3 and 2.4 Hz; 5,5′ of b$(NH_2)_2$); 5.8 (4 H, s, $NH_2$).

**[(4,4′-$(Me)_2$-bpy)$(CO)_3Re^I$(4,4′-bpy)$Re^I(CO)_3$(bpy)]$(PF_6)_2$.** The same procedure was utilized as for the previous complex, giving 53 mg (0.04 mmol) of a yellow solid. The yield was 24% vs [$((Me)_2$-bpy)-$(CO)_3Re^I$(4,4′-bpy)]$(PF_6)$. Anal. Calcd for $C_{38}H_{28}N_6O_6Re_2P_2F_{12}$: C, 34.39; H, 2.12; N, 6.33; P, 4.67. Found: C, 34.47; H, 2.34; N, 6.17; P, 4.47. $^1$H NMR, ppm: 9.2 (2 H; d, 5.1 Hz; 6,6′ of b); 9.02 (2 H; d, 5.1 Hz; 6,6′ of b$(Me)_2$); 8.6–8.3 (8 H; m; 4,4′ and 3,3′ of b and 2,2′ and 6,6′ of 4,4′-bpy); 8.21 (2 H; s; 3,3′ of b$(Me)_2$); 7.7 (2 H; d of d, 5.3 and 1.3 Hz; 5,5′ of b); 7.58 (2 H; d of d, 5.1 and 1.6 Hz; 5,5′ of b$(Me)_2$); 7.45 (4 H; d of d, 5.3 and 1.4 Hz; 3,3′ and 5,5′ of 4,4′-bpy); 2.54 (6 H; s; $CH_3$).

**[(4,4′-$(NH_2)_2$-bpy)$(CO)_3Re^I$(4,4′-bpy)$Re^I(CO)_3$(4,4′-$(CO_2Et)_2$-bpy)]$(PF_6)_2$.** This salt was obtained by the reaction between 180 mg (0.2 mmol) of [(4,4′-$(CO_2Et)_2$-bpy)$(CO)_3Re^I$(4,4′-bpy)]$(PF_6)$ and 300 mg (0.5 mmol) of [(4,4′-$(NH_2)_2$-bpy)$(CO)_3Re^I$(TFMS)] in 10 mL of THF heated at reflux overnight. A yellow precipitate was isolated following addition to ether. It was filtered and washed with ether. After the precipitate was dissolved in acetone, the resulting solution was added to an aqueous solution of $[NH_4](PF_6)$, which gave a yellow precipitate. The solid material was chromatographed on silica gel (75–230 mesh) with 1:2 (v/v) acetonitrile/methylene chloride. The final purification was achieved by flash chromatography on silica gel (15 μm) with 1:2 (v/v) acetonitrile/methylene chloride and 1:10 (v/v) acetone/water (0.05 M $[NH_4](PF_6)$). The product was dried, dissolved in acetonitrile, and reprecipitated by adding to ether. The yield was 45%, 133 mg (0.09 mmol). Anal. Calcd for $C_{42}H_{34}N_8O_{10}Re_2P_2F_{12}$: C, 34.24; H, 2.31; N, 7.61; P, 4.21. Found: C, 33.63; H, 2.43; N, 7.43;, P, 4.00. $^1$H NMR, ppm: 9.4 (2 H; d of d, 5.7 and 0.5 Hz; 6,6′ of b$(CO_2Et)_2$); 8.87 (2 H; d, 0.5 Hz; 3,3′ of b$(CO_2Et)_2$); 8.49 (2 H; d of d, 6.4 and 0.9 Hz; 6,6′ of b$(NH_2)_2$); 8.31 (2 H; d, 2.2 Hz; 2 and 6 of 4,4′-bpy); 8.29 (2 H; d, 2.2 Hz; 2′ and 6′ of 4,4′-bpy); 8.20 (2 H; d of d, 5.7 and 1.5 Hz; 5,5′ of b$(CO_2Et)_2$); 7.50 (4 H; d of d, 5.2 and 1.5 Hz; 3,3′ and 5,5′ of 4,4′-bpy); 7.20 (2 H; d of d, 6.4 and 3.4 Hz; 3,3′ of b$(NH_2)_2$); 5.86 (4 H; s; $NH_2$), 4.44 (8 H; q, 7.1 Hz; $OCH_2CH_3$); 1.41 (12 H; t, 7.1 Hz; $OCH_2CH_3$).

**[(bpy)$(CO)_3Re^I$(4,4′-bpy)$Re^I(CO)_3$(4,4′-$(CO_2Et)_2$-bpy)]$(PF_6)_2$.** The same procedure was utilized as for the previous complex, giving 75 mg (0.052 mmol) of a yellow solid. The yield was 32.5%. Anal. Calcd for

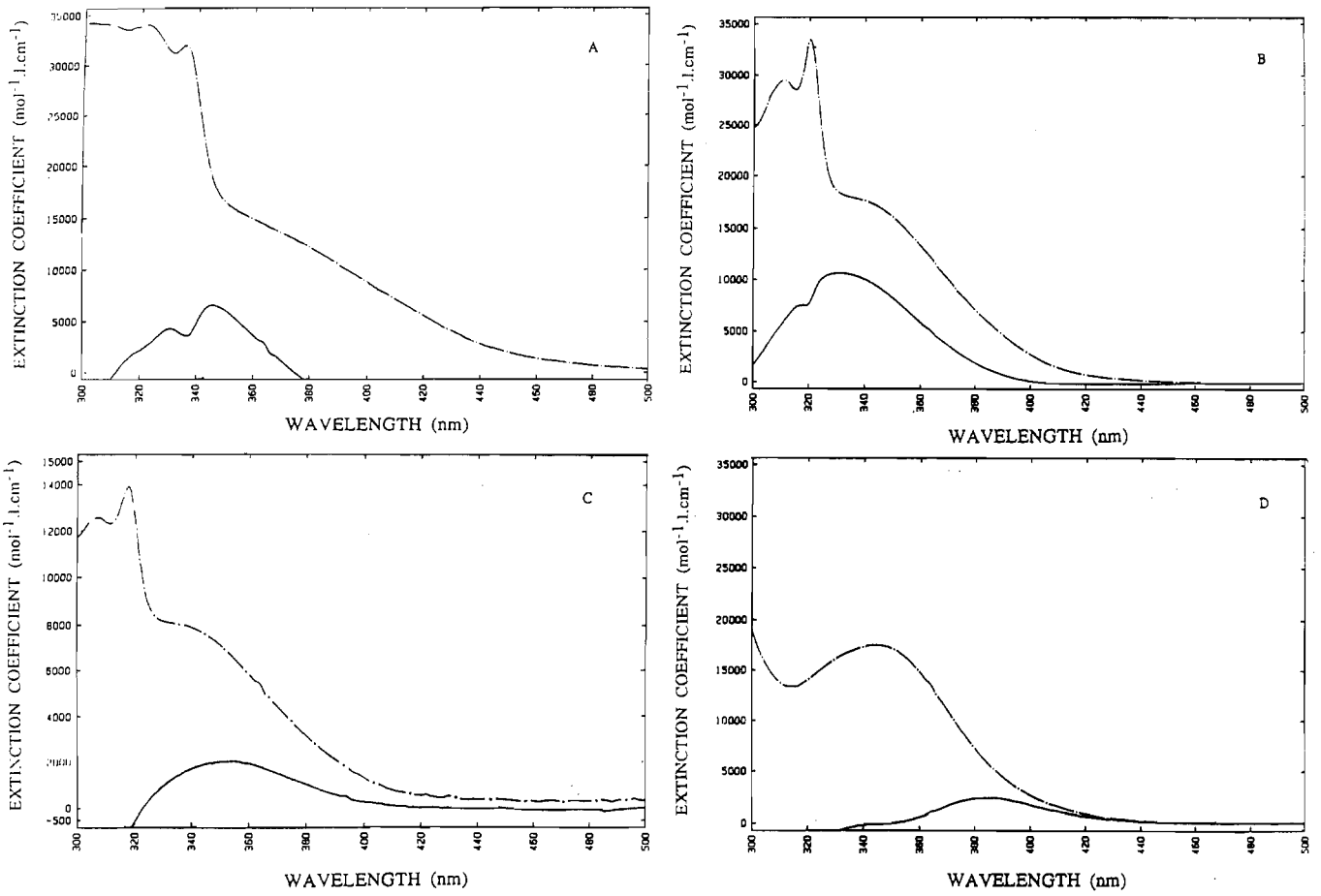


**Figure 1.** (-·-) Absorption spectra in $CH_3CN$ of the symmetrical ligand-bridged complexes (A) $[(b(CO_2Et)_2)(CO)_3Re^I(4,4'\text{-bpy})Re^I(CO)_3(b(CO_2Et)_2)]^{2+}$, (B) $[(b)(CO)_3Re^I(4,4'\text{-bpy})Re^I(CO)_3(b)]^{2+}$, (C) $[(b(Me)_2)(CO)_3Re^I(4,4'\text{-bpy})Re^I(CO)_3(b(Me)_2)]^{2+}$, and (D) $[(b(NH_2)_2)(CO)_3Re^I(4,4'\text{-bpy})Re^I(CO)_3(b(NH_2)_2)]^{2+}$. (—) Difference spectra between the ligand-bridged complexes and the doubled spectra of the corresponding 4-Etpy complexes, showing the $d\pi \rightarrow \pi^*(4,4'\text{-bpy})$ transitions.

$C_{42}H_{32}N_6O_{10}Re_2P_2F_{12}$: C, 34.95; H, 2.22; N, 5.82; F, 15.81. Found: C, 34.01; H, 2.30; N, 5.63; F, 15.32. $^1$H NMR, ppm: 9.4 (2 H; d of d, 5.7 and 0.5 Hz; 6,6′ of $b(CO_2Et)_2$); 9.2 (2 H; d, 5.6 Hz; 6,6′ of b); 8.9 (2 H; d, 1 Hz; 3,3′ of $b(CO_2Et)_2$); 8.45 (2 H; d, 5.9 Hz; 3,3′ of b); 8.31 (2 H; d, 2.2 Hz; 2 and 6 of 4,4′-bpy); 8.25–8.15 (6 H; 2′ and 6′ of 4,4′-bpy and 4,4′ of b and $b(CO_2Et)_2$) 7.8 (2 H; d of d, 5.2 and 1.4 Hz; 5,5′ of b); 7.56 (4 H; d of d, 5.3 and 1.2 Hz; 5,5′ and 3,3′ of 4,4′-bpy); 4.44 (8 H; q, 7.1 Hz; $OCH_2CH_3$); 1.41 (12 H; t, 7.1 Hz; $OCH_2CH_3$).

**$[(bpy)(CO)_3Re^I(3,3'\text{-}(Me)_2\text{-}4,4'\text{-bpy})Re^I(CO)_3(4,4'\text{-}(CO_2Et)_2\text{-bpy})](PF_6)_2$.** A quantity of 0.12 mmol of $[(bpy)(CO)_3Re^I(3,3'\text{-}(Me)_2\text{-}4,4'\text{-bpy})](PF_6)$ and 0.28 mmol of $[(4,4'\text{-}(CO_2Et)_2\text{-bpy})(CO)_3Re^I(CF_3SO_3)]$ were heated at gentle reflux for 4 h in 10 mL of THF. Ether was slowly added, and the resulting yellow/orange precipitate was collected and dried under vacuum. After the counterion for $PF_6^-$ was exchanged by adding it to a saturated aqueous solution of $[NH_4](PF_6)$, the solid material was chromatographed on silica gel first with 1:2 (v/v) $CH_3CN/CH_2Cl_2$ as a starting eluent followed by 10:1 (v/v) acetone/water, 0.05 M in $[NH_4](PF_6)$. It was eluted a second time by using 1:4 (v/v) $CH_3CN/CH_2Cl_2$ followed by 10:1 (v/v) acetone/water, 0.05 M in $[NH_4](PF_6)$. The eluent was evaporated and the solid dissolved in $CH_3CN$ and reprecipitated by slow addition of ethyl ether. The yellow/orange precipitate was collected, washed, and dried under vacuum to give 67 mg (0.045 mmol); the yield was 38%. Anal. Calcd for $C_{44}H_{36}N_6O_{10}Re_2P_2F_{12}$: C, 35.92; H, 2.45; N, 5.71. Found: C, 35.83; H, 2.48; N, 5.73. $^1$H NMR, ppm: 9.4 (2 H; d of d, 5.7 and 0.5 Hz; 6,6′ of $b(CO_2Et)_2$); 9.2 (2 H; d, 5.6 Hz; 6,6′ of b); 8.9 (2 H; d, 1 Hz; 3,3′ of $b(CO_2Et)_2$); 8.45 (2 H; d, 5.9 Hz; 3,3′ of b); 8.3–8.1 (6 H; m; 2,2′ and 6,6′ of 4,4′-bpy and 5,5′ of $b(CO_2Et)_2$); 8.01 (2 H; d, 2.2 Hz; 2 and 6 of 4,4′-bpy); 7.76 (2 H; d, 5.6 Hz; 5,5′ of b); 6.8 and 6.75 (4 H; d of d, 1 and 2.6 Hz; 5 and 5′ of $(Me)_2$-4,4′-bpy); 4.44 (8 H; q, 7.1 Hz; $OCH_2CH_3$); 2.91 (6 H; s; $CH_3$ of $(Me)_2$-4,4′-bpy); 1.41 (12 H; t, 7.1 Hz; $OCH_2CH_3$).

## Results

**Electrochemistry.** Reduction potentials obtained by cyclic voltammetry for a series of complexes in acetonitrile are collected in Table I. In the cyclic voltammograms, a series of three waves generally appear over the potential range −1.6 to +2.2 V (vs SSCE). The $E_{1/2}$ values derived from the cyclic voltammograms and the assignments of the redox processes involved are summarized in Table I. Because of reactions with water and/or impurities in the solvent, the Re(II/I) waves are irreversible with only the oxidative peak potential being well-defined. Reductive components are observed for these waves when the oxidizing strength of the Re(II/I) couple is decreased and at higher scan rates (0.5 or 1 V/s). This has been noted by other groups as well.[9c,e]

In the symmetrical ligand-bridged complexes, this wave and the $bpy^{0/-}$ reduction waves are two-electron processes. The splittings between the two one-electron Re(II/I) or $bpy^{0/-}$ couples are too small to resolve. This is an expected result for complexes such as these where both electronic coupling and electrostatic interactions are expected to be small.[14] The two-electron character of these waves is shown by their integrated areas and by the appearace of two one-electron waves for the Re(II/I) and $bpy^{0/-}$ couples in the unsymmetrical complexes.

**Absorption Spectra.** The absorption spectra of these complexes are characterized by a series of MLCT and $\pi \rightarrow \pi^*(b(X)_2)$ transitions.[15] In this coordination environment, the MLCT transitions are at high energy and overlap with ligand-centered $\pi \rightarrow \pi^*(b(X)_2)$ transitions. Representative absorption spectra are shown in Figures 1 and 2. Band maxima and their assignments are presented in Table IIA for the symmetrical ligand-

(14) (a) Sutton, S. E.; Taube, H. *Inorg. Chem.* **1981**, *20*, 3125. (b) Sutton, S. E.; Sutton, D. M.; Taube, H. *Inorg. Chem.* **1979**, *18*, 1017. (c) Callahan, R. W.; Brown, G. M.; Meyer, T. J. *Inorg. Chem.* **1975**, *14*, 1443. (d) Sokol, W. F.; Evans, D. H. *J. Electroanal. Chem.* **1980**, *108*, 107.

(15) (a) Giordano, P. J.; Wrighton, M. S. *J. Am. Chem. Soc.* **1979**, *101*, 2888. (b) Sullivan, B. P. *J. Phys. Chem.* **1989**, *93*, 24.

**Table I.** $E_{1/2}$ Values in Volts vs SSCE at 293 ± 2 K in 0.1 M $[N(n\text{-}C_4H_9)_4](PF_6)/CH_3CN$[a]

| complex | oxidn $E_{p,a}$,[b] V $Re^{II/I}$ | redn $E_{1/2}$,[c] V $(4,4'\text{-bpy})^{0/-}$ | $(bpy^{0/-})_1$ | $(bpy^{0/-})_2$ |
|---|---|---|---|---|
| $[(b(NH_2)_2)(CO)_3Re(4\text{-Etpy})]^+$ | +1.58 | | −1.65[f] | |
| $[(b(NH_2)_2)(CO)_3Re(4,4'\text{-bpy})Re(CO)_3(b(NH_2)_2)]^{2+}$ | +1.62[d] | −1.09 | −1.65[e,f] | |
| $[(b(Me)_2)(CO)_3Re(4,4'\text{-bpy})]^+$ | +1.85 | | −1.33[f] | |
| $[(b(Me)_2)(CO)_3Re(4,4'\text{-bpy})Re(CO)_3(b(Me)_2)]^{2+}$ | +1.85[d] | −1.04 | −1.3[f] | |
| $[(b)(CO)_3Re(4\text{-Etpy})]^+$ | +1.85 | | −1.17 | |
| $[(b)(CO)_3Re(bpa)Re(CO)_3(b)]^{2+}$ | +1.85[d] | | −1.17[e] | |
| $[(b)(CO)_3Re(4,4'\text{-bpy})Re(CO)_3(b)]^{2+}$ | +1.90[d] | −1.06 | −1.20[e] | |
| $[(b(CO_2Et)_2)(CO)_3Re(4\text{-Etpy})]^+$ | +1.95 | | −0.87 | −1.18[h] |
| $[(b(CO_2Et)_2)(CO)_3Re(4,4'\text{-bpy})Re(CO)_3(b(CO_2Et)_2)]^{2+}$ | +2.0[d,g] | −1.25[f] | −0.82 | −1.18 |
| $[(b(NH_2)_2)(CO)_3Re(4,4'\text{-bpy})Re(CO)_3(b)]^{2+}$ | +1.64, +1.9 | −1.06 | −1.21 | −1.62[f] |
| $[(b(NH_2)_2)(CO)_3Re(4,4'\text{-bpy})Re(CO)_3(b(CO_2Et)_2]^{2+}$ | +1.64, +2.0[g] | −1.15 | −0.82 | −1.63[f] |
| $[(b(Me)_2)(CO)_3Re(4,4'\text{-bpy})Re(CO)_3(b)]^{2+}$ | +1.92[d] | −1.05 | −1.2 | −1.34[f] |
| $[(b)(CO)_3Re(4,4'\text{-bpy})Re(CO)_3(b(CO_2Et)_2]^{2+}$ | +1.90, +2.0[g] | −1.20[h] | −0.80 | −1.20[h] |
| $[(b)(CO)_3Re(3,3'\text{-}(Me)_2\text{-}4,4'\text{-bpy})Re(CO)_3(b(CO_2Et)_2)]^{2+}$ | +1.90 | | −0.82 | −1.17 |

[a] From cyclic voltammetric measurements by using a platinum working electrode at a scan rate of 0.1 V/s vs SSCE. [b] The couples are chemically irreversible. The potentials cited are oxidative peak potentials, $E_{p,a}$. See the text for details. [c] Calculated as the midpoint between peak potentials for the oxidative and reductive waves. [d] For the symmetrical ligand-bridged complexes, the difference in peak potentials for the two Re(II/I) oxidative processes are irresolvable. [e] For the symmetrical ligand-bridged complexes, the separate bpy-based reduction waves are irresolvable. [f] Irreversible wave (the peak current for the oxidative wave is less than the reductive peak current). [g] This wave appears as a shoulder in the solvent background. [h] At the second wave, one-electron reduction occurs at both 2,2'-bpy and 4,4'-bpy.

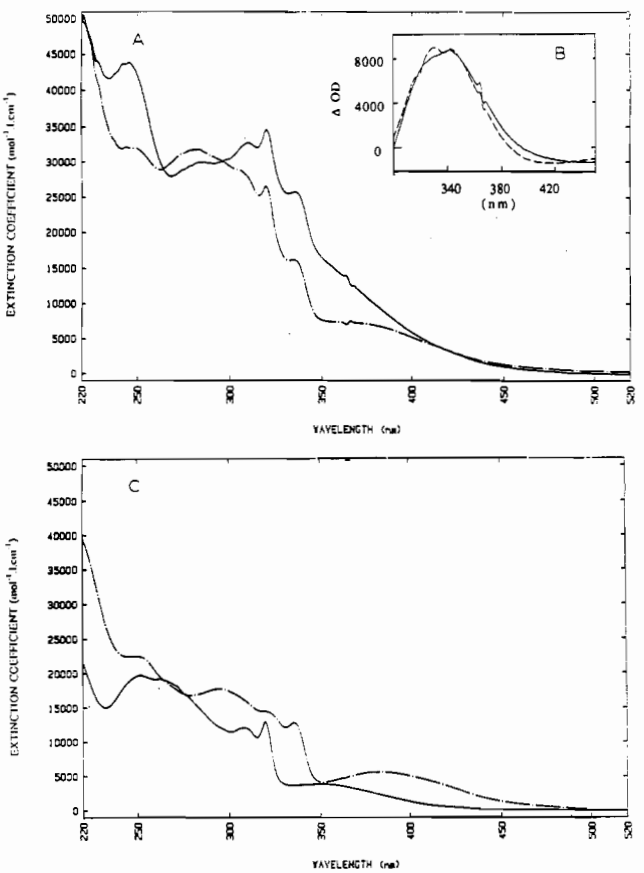


**Figure 2.** (A) Absorption spectra in $CH_3CN$ for $[(b)(CO)_3Re^I(4,4'\text{-bpy})Re^I(CO)_3(b(CO_2Et)_2)]^{2+}$ (—) and $[(b)(CO)_3Re^I(3,3'\text{-}(Me)_2\text{-}4,4'\text{-bpy})Re^I(CO)_3(b(CO_2Et)_2)]^{2+}$ (-·-). (B) Difference spectra in $CH_3CN$, showing the $d\pi \rightarrow \pi^*(4,4'\text{-bpy})$ MLCT transition in $[(b)(CO)_3Re^I\text{-}(4,4'\text{-bpy})Re^I(CO)_3(b(CO_2Et)_2)]^{2+}$ obtained by subtracting the spectrum of this complex from that of the $3,3'\text{-}(Me)_2\text{-}4,4'$-bpy ligand-bridged complex (—) or from twice the spectrum of the 4-Etpy complex (-·-). (C) Absorption spectra in $CH_3CN$ for $[(b)(CO)_3Re^I(4\text{-Etpy})]^+$ (—) and $[(b(CO_2Et)_2)(CO)_3Re^I(4\text{-Etpy})]^+$ (-·-).

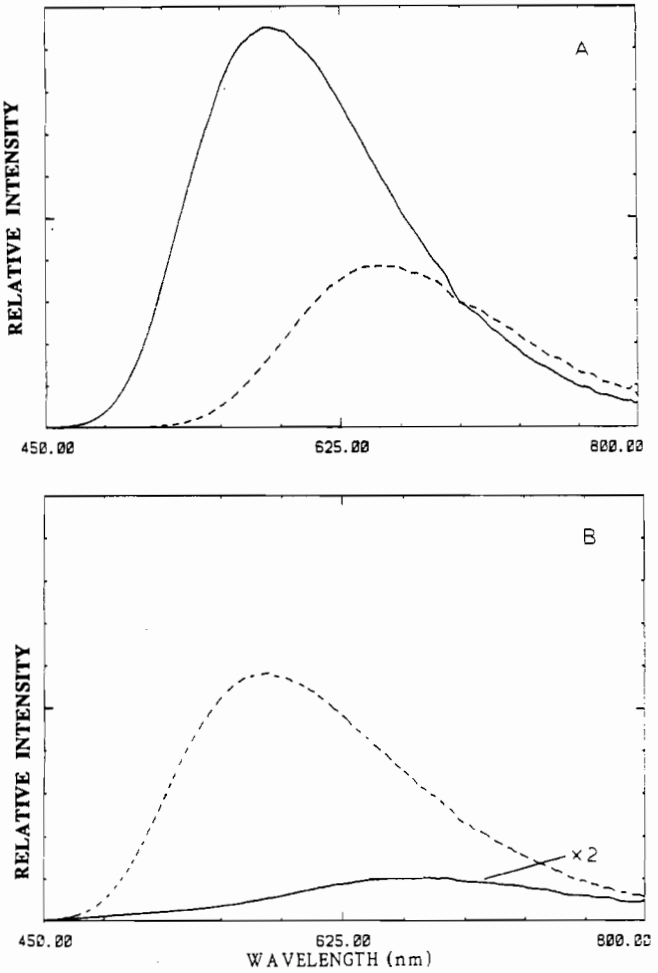


**Figure 3.** Normalized emission spectra obtained at absorbance 0.1 in $CH_3CN$ at 293 ± 2 K following excitation at 380 nm for (A) $[(b\text{-}(CO_2Et)_2)(CO)_3Re^I(4,4'\text{-bpy})Re^I(CO)_3(b(CO_2Et)_2)]^{2+}$ (--) and $[(b)\text{-}(CO)_3Re^I(4,4'\text{-bpy})Re^I(CO)_3(b)]^{2+}$ (—) and (B) $[(b(NH_2)_2)\text{-}(CO)_3Re^I(4,4'\text{-bpy})Re^I(CO)_3(b(NH_2)_2]^{2+}$ (×2) (—) and $[(b(Me)_2)\text{-}(CO)_3Re^I(4,4'\text{-bpy})Re^I(CO)_3(b(Me)_2)]^{2+}$ (--).

bridged complexes and related 4-Etpy complexes and in Table IIB for the unsymmetrical ligand-bridged complexes.

The extent of overlap between the $\pi \rightarrow \pi^*$ and MLCT transitions depends upon the electronic character of the bpy substituents. With X = $NH_2$, the bpy localized $\pi \rightarrow \pi^*$ transition is shifted to sufficiently high energy that the MLCT manifold can be discerned clearly. Also shown in Figure 1 are difference spectra that were calculated in order to deconvolute the $d\pi(Re) \rightarrow \pi^*\text{-}(b(X)_2)$ bands from $d\pi(Re) \rightarrow \pi^*(4,4'\text{-bpy})$ bands. In Figure 2 are shown spectra and difference spectra for the unsymmetrical complexes $[(b)(CO)_3Re^I(L)Re^I(CO)_3(b(CO_2Et)_2)]^{2+}$ with L = 4,4'-bpy or 3,3'-dimethyl-4,4'-bpy and the related monomers, $[(b)Re^I(CO)_3(4\text{-Etpy})]^+$ and $[(b(CO_2Et)_2)Re^I(CO)_3(4\text{-Etpy})]^+$.

**Table II.** UV–Visible Absorption Maxima and Band Assignments in $CH_3CN$ at 293 ± 2K[a]

| complex | $\lambda_{max}$, nm | $10^{-3}\ \epsilon$, $mol^{-1}\cdot L\cdot cm^{-1}$ | assignment |
|---|---|---|---|
| A. Symmetrical Ligand-Bridged Complexes and Related 4-Etpy Complexes | | | |
| $[(b(NH_2)_2)(CO)_3Re(4\text{-Etpy})]^+$ | 344 | 8.8 | $d\pi \rightarrow \pi^*((NH_2)_2\text{-bpy})$ |
| | 256 | 19.7 | $\pi \rightarrow \pi^*((NH_2)_2\text{-bpy})$ |
| $[(b(NH_2)_2)(CO)_3Re(4,4'\text{-bpy})Re(CO)_3(b(NH_2)_2)]^{2+}$ | 345 | 17.5 | $d\pi \rightarrow \pi^*((NH_2)_2\text{-bpy})$; (4,4′-bpy) |
| | 285[b] | 36.2 | $\pi \rightarrow \pi^*((NH_2)_2\text{-bpy})$ |
| $[(b(Me)_2)(CO)_3Re(4,4'\text{-bpy})]^+$ | 340 | 6.2 | $d\pi \rightarrow \pi^*((Me_2\text{-bpy})$ |
| | 318 | 14.8 | $\pi \rightarrow \pi^*$ |
| | 306 | 14.9 | $\pi \rightarrow \pi^*$ |
| | 246 | 25.2 | $\pi \rightarrow \pi^*$ |
| $[(b(Me)_2)(CO)_3Re(4,4'\text{-bpy})Re(CO)_3(b(Me)_2)]^{2+}$ | 340 | 18.8 | $d\pi \rightarrow \pi^*((Me)_2\text{-bpy})$; (4,4′-bpy) |
| | 318 | 33.3 | $\pi \rightarrow \pi^*$ |
| | 306 | 29.8 | $\pi \rightarrow \pi^*$ |
| | 245 | 44.7 | $\pi \rightarrow \pi^*$ |
| $[(b)(CO)_3Re(4\text{-Etpy})]^+$ | 352 | 3.9 | $d\pi \rightarrow \pi^*$(bpy) |
| | 320 | 12.9 | $\pi \rightarrow \pi^*$ |
| | 308 | 12.0 | $\pi \rightarrow \pi^*$ |
| | 265[b] | 19.1 | $\pi \rightarrow \pi^*$ |
| | 252 | 19.7 | $\pi \rightarrow \pi^*$ |
| $[(b)(CO)_3Re(bpa)Re(CO)_3(b)]^{2+}$ | 352 | 6.7 | $d\pi \rightarrow \pi^*$(bpy) |
| | 320 | 21.5 | $\pi \rightarrow \pi^*$ |
| | 308 | 22.2 | $\pi \rightarrow \pi^*$ |
| | 268 | 33.9 | $\pi \rightarrow \pi^*$ |
| | 252 | 33.5 | $\pi \rightarrow \pi^*$ |
| $[(b)(CO)_3Re(4,4'\text{-bpy})Re(CO)_3(b)]^{2+}$ | 340 | 17.6 | $d\pi \rightarrow \pi^*$(bpy); (4,4′-bpy) |
| | 320 | 33.4 | $\pi \rightarrow \pi^*$ |
| | 310 | 29.4 | $\pi \rightarrow \pi^*$ |
| | 275[b] | 28.4 | $\pi \rightarrow \pi^*$ |
| | 246 | 40.8 | $\pi \rightarrow \pi^*$ |
| $[(b(CO_2Et)_2)(CO)_3Re(4\text{-Etpy})]^+$ | 385 | 5.7 | $d\pi \rightarrow \pi^*((CO_2Et)_2\text{-bpy})$ |
| | 336 | 12.8 | $d\pi \rightarrow \pi^*((CO_2Et)_2\text{-bpy})$ |
| | 325 | 15.3 | $\pi \rightarrow \pi^*$ |
| | 294 | 17.7 | $\pi \rightarrow \pi^*$ |
| | 244 | 22.5 | $\pi \rightarrow \pi^*$ |
| $[(b(CO_2Et)_2)(CO)_3Re(4,4'\text{-bpy})Re(CO)_3(b(CO_2Et)_2)]^{2+}$ | 350 | 16.5 | $d\pi \rightarrow \pi^*((CO_2Et)_2\text{-bpy})$; (4,4′-bpy) |
| | 336 | 31.9 | $d\pi \rightarrow \pi^*((CO_2Et)_2\text{-bpy})$; (4,4′-bpy) |
| | 322[b] | 34.0 | $\pi \rightarrow \pi^*$ |
| | 304 | 34.2 | $\pi \rightarrow \pi^*$ |
| | 244 | 39.9 | $\pi \rightarrow \pi^*$ |
| B. Unsymmetrical Ligand-Bridged Complexes | | | |
| $[(b(NH_2)_2)(CO)_3Re(4,4'\text{-bpy})Re(CO)_3(b(CO_2Et)_2)]^{2+}$ | 350 | 16.4 | $d\pi \rightarrow \pi^*((CO_2Et)_2\text{-bpy})$; $((NH_2)_2\text{-bpy})$; ((4,4′-bpy) |
| | 336 | 23.8 | $d\pi \rightarrow \pi^*((CO_2Et)_2\text{-bpy})$; $((NH_2)_2\text{-bpy})$; (4,4′-bpy) |
| | 322 | 24.2 | $\pi \rightarrow \pi^*$ |
| | 290[b] | 34.4 | $\pi \rightarrow \pi^*$ |
| | 252 | 59.5 | $\pi \rightarrow \pi^*((NH_2)_2\text{-bpy})$ |
| $[(b(NH_2)_2)(CO)_3Re(4,4'\text{-bpy})Re(CO)_3(b)]^{2+}$ | 340 | 19.7 | $d\pi \rightarrow \pi^*$(bpy); $((NH_2)_2\text{-bpy})$; (4,4′-bpy) |
| | 320 | 25.6 | $\pi \rightarrow \pi^*$ |
| | 310 | 23.9 | $\pi \rightarrow \pi^*$ |
| | 268[b] | 44.3 | $\pi \rightarrow \pi^*$ |
| | 250 | 48.4 | $\pi \rightarrow \pi^*((NH_2)_2\text{-bpy})$ |
| $[(b(Me)_2)(CO)_3Re(4,4'\text{-bpy})Re(CO)_3(b)]^{2+}$ | 340 | 17.9 | $d\pi \rightarrow \pi^*$(bpy); $(Me_2\text{-bpy})$; (4,4′-bpy) |
| | 318 | 31.1 | $\pi \rightarrow \pi^*$ |
| | 308 | 28.2 | $\pi \rightarrow \pi^*$ |
| | 270[b] | 30.5 | $\pi \rightarrow \pi^*$ |
| | 246 | 43.4 | $\pi \rightarrow \pi^*$ |
| $[(b)(CO)_3Re(4,4'\text{-bpy})Re(CO)_3(b(CO_2Et)_2)]^{2+}$ | 380 | 9.1 | $d\pi \rightarrow \pi^*$(bpy); $((CO_2Et)_2\text{-bpy})$; (4,4′-bpy) |
| | 350 | 15.9 | $d\pi \rightarrow \pi^*$(bpy); $((CO_2Et)_2\text{-bpy})$; (4,4′-bpy) |
| | 336 | 25.1 | $d\pi \rightarrow \pi^*$(bpy); $((CO_2Et)_2\text{-bpy})$; (4,4′-bpy) |
| | 320 | 33.9 | $\pi \rightarrow \pi^*$ |
| | 280 | 28.8 | $\pi \rightarrow \pi^*$ |
| | 250 | 41.6 | $\pi \rightarrow \pi^*$ |
| $[(b)(CO)_3Re(3,3'\text{-}(CH_3)_2\text{-}4,4'\text{-bpy})Re(CO)_3(b(CO_2Et)_2)]^{2+}$ | 380 | 7.3 | $d\pi \rightarrow \pi^*$(bpy); $((CO_2Et)_2\text{-bpy})$ |
| | 350 | 8.1 | $d\pi \rightarrow \pi^*$(bpy); $((CO_2Et)_2\text{-bpy})$ |
| | 336 | 16.6 | $d\pi \rightarrow \pi^*$(bpy); $((CO_2Et)_2\text{-bpy})$ |
| | 320 | 27.0 | $\pi \rightarrow \pi^*$ |
| | 308 | 28.7 | $\pi \rightarrow \pi^*$ |
| | 280 | 32.2 | $\pi \rightarrow \pi^*$ |
| | 250 | 32.4 | $\pi \rightarrow \pi^*$ |

[a] $\lambda_{max}$ is ±2 nm and $\epsilon$ is ±5%. [b] Shoulder.

**Emission Spectra. 294 ± 1 K.** In Figure 3A are shown room-temperature emission spectra for $[(b)(CO)_3Re^I(4,4'\text{-bpy})Re^I(CO)_3(b)]^{2+}$ and $[(b(CO_2Et)_2)(CO)_3Re^I(4,4'\text{-bpy})Re^I(CO)_3(b(CO_2Et)_2)]^{2+}$ and in Figure 3B for $[(b(Me)_2)(CO)_3Re^I(4,4'\text{-bpy})Re^I(CO)_3(b(Me)_2)]^{2+}$ and $[(b(NH_2)_2)(CO)_3Re^I(4,4'\text{-bpy})Re^I(CO)_3(b(NH_2)_2)]^{2+}$. The spectra were acquired from solutions of equal absorbance (OD = 0.1) at the excitation wavelength. Emission from $[(b(NH_2)_2)(CO)_3Re^I(4,4'\text{-bpy})Re^I(CO)_3(b(NH_2)_2)]^{2+}$ is noticeably red-shifted and decreased in intensity compared to the others. Emission spectra

**Table III.** Emission Quantum Yields and Maxima at 293 ± 2 K[a]

| complex | $CH_3CN$ | | PC | | DCE | |
|---|---|---|---|---|---|---|
| | $10^2\Phi_{em}$ | $\lambda_{max}$, nm | $10^2\Phi_{em}$ | $\lambda_{max}$, nm | $\Phi_{em}$ | $\lambda_{max}$, nm |
| $[(b(NH_2)_2)(CO)_3Re(4\text{-}Etpy)]^+$ | 25.2 | 531 | 9.81 | 534 | 27.1 | 530 |
| $[(b(NH_2)_2)(CO)_3Re(4,4'\text{-}bpy)Re(CO)_3(b(NH_2)_2)]^{2+}$ | 0.07 | 660[b] | 0.06 | 650[b] | 0.15 | 610 |
| $[(b(Me)_2)(CO)_3Re(4,4'\text{-}bpy)]^+$ | 4.40 | 580 | 4.65 | 575 | 18.7 | 565 |
| $[(b(Me)_2)(CO)_3Re(4,4'\text{-}bpy)Re(CO)_3(b(Me)_2)]^{2+}$ | 0.94 | 585[c] | 0.68 | 585[c] | 9.0 | 565 |
| $[(b)(CO)_3Re(4\text{-}Etpy)]^+$ | 2.70 | 590 | 3.05 | 596 | 13.5 | 575 |
| $[(b)(CO)_3Re(bpa)Re(CO)_3(b)]^{2+}$ | 3.25 | 590 | 2.64 | 596 | 13.5 | 575 |
| $[(b)(CO)_3Re(4,4'\text{-}bpy)Re(CO)_3(b)]^{2+}$ | 3.32 | 585 | 2.67 | 590 | 17.0 | 570 |
| $[(b(CO_2Et)_2)(CO)_3Re(4\text{-}Etpy)]^+$ | 0.77 | 660 | | | | |
| $[(b(CO_2Et)_2)(CO)_3Re(4,4'\text{-}bpy)Re(CO)_3(b(CO_2Et)_2)]^{2+}$ | 1.19 | 650 | 1.02 | 650 | 8.5 | 625 |
| $[(b(NH_2)_2)(CO)_3Re(4,4'\text{-}bpy)Re(CO)_3(b)]^{2+}$ | 0.42 | 605[d] | 0.19 | 598 | 2.0 | 590 |
| $[(b(NH_2)_2)(CO)_3Re(4,4'\text{-}bpy)Re(CO)_3(b(CO_2Et)_2)]^{2+}$ | 1.02 | 650 | 0.50 | 650 | 6.0 | 620 |
| $[(b(Me)_2)(CO)_3Re(4,4'\text{-}bpy)Re(CO)_3(b)]^{2+}$ | 2.24 | 585 | 1.99 | 585 | 14.5 | 570[d] |
| $[(b)(CO)_3Re(4,4'\text{-}bpy)Re(CO)_3(b(CO_2Et)_2)]^{2+}$ | 1.19 | 650 | 1.02 | 650 | 9.5 | 625 |
| $[(b)(CO)_3Re(3,3'\text{-}(CH_3)_2\text{-}4,4'\text{-}bpy)Re(CO)_3(b(CO_2Et)_2)]^{2+}$[e] | 1.85 | 620[f] | 1.41 | 630[f] | 16.0 | 612[f] |

[a] The excitation wavelength was 380 nm. The uncertainties are ±3 nm in $\lambda_{max}$ and ±10% in $\Phi_{em}$. PC is propylene carbonate and DCE is 1,2-dichloroethane. [b] Broad peak, ±10 nm. [c] Broad peak, ±5 nm. [d] Excitation wavelength dependent. The wavelength dependence appears to be a consequence of the appearance of decomposition photoproducts. [e] The bridging ligand is 3,3'-dimethyl-4,4'-bipyridine. [f] Excitation wavelength dependent. See text for details.

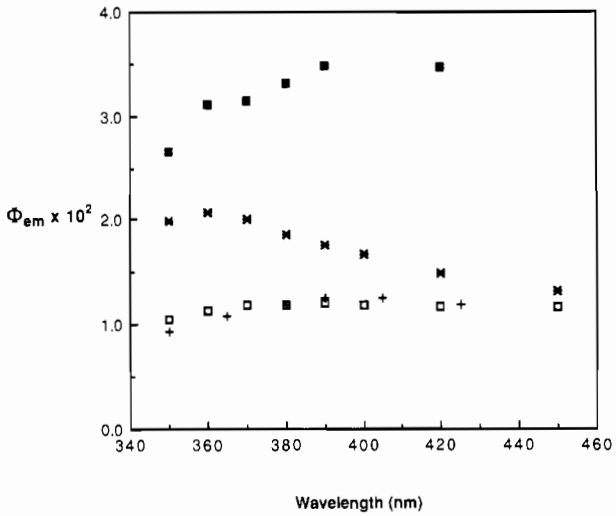


**Figure 4.** Wavelength dependence of $\Phi_{em}$ in $CH_3CN$ at 293 ± 2 K: $[(b(CO_2Et)_2)(CO)_3Re^I(4,4'\text{-}bpy)Re^I(CO)_3(b(CO_2Et)_2)]^{2+}$ (+), $[(b)(CO)_3Re^I(4,4'\text{-}bpy)Re^I(CO)_3(b)]^{2+}$ (■), $[(b)(CO)_3Re^I(4,4'\text{-}bpy)Re^I(CO)_3(b(CO_2Et)_2)]^{2+}$ (□), and $[(b)(CO)_3Re^I(3,3'\text{-}(Me)_2\text{-}4,4'\text{-}bpy)Re^I(CO)_3(b(CO_2Et)_2)]^{2+}$ (×).

for $[(b)(CO)_3Re^I(4,4'\text{-}bpy)Re^I(CO)_3(b(CO_2Et)_2)]^{2+}$, $[(b(NH_2)_2)(CO)_3Re^I(4,4'\text{-}bpy)Re^I(CO)_3(b(CO_2Et)_2)]^{2+}$, $[(b(CO_2Et)_2)(CO)_3Re^I(4,4'\text{-}bpy)Re^I(CO)_3(b(CO_2Et)_2)]^{2+}$, and $[(b)(CO)_3Re^I(4,4'\text{-}bpy)Re^I(CO)_3(b)]^{2+}$ are slightly excitation wavelength dependent, Figure 4. The emission spectral profiles remain the same but the emission quantum yield increases slightly as the excitation energy is decreased. The wavelength-dependent behavior is observed in propylene carbonate (PC), but in 1,2-dichloroethane (DCE), the quantum yields are nearly wavelength-independent.

Emission from $[(b(NH_2)_2)(CO)_3Re^I(4,4'\text{-}bpy)Re^I(CO)_3(b(CO_2Et)_2)]^{2+}$ is essentially superimposable in band shape and maximum with emission from $[(b)(CO)_3Re^I(4,4'\text{-}bpy)Re^I(CO)_3(b(CO_2Et)_2)]^{2+}$. For the bpa-bridged complex, $[(b)(CO)_3Re^I(bpa)Re^I(CO)_3(b)]^{2+}$, the emission spectral profile and $\Phi_{em}$ are essentially superimposable with those of the $[(b)(CO)_3Re^I(4\text{-}Etpy)]^+$. In both, $\Phi_{em}$ is excitation wavelength independent.

For $[(b)(CO)_3Re^I(3,3'\text{-}(CH_3)_2\text{-}4,4'\text{-}bpy)Re^I(CO)_3(b(CO_2Et)_2)]^{2+}$, both the band shape and $\Phi_{em}$ are excitation wavelength dependent. An emission spectrum obtained following excitation at 380 nm is compared in Figure 5A with spectra obtained for the complexes $[(b)(CO)_3Re^I(4\text{-}Etpy)]^+$ and $[(b(CO_2Et)_2)(CO)_3Re^I(4\text{-}Etpy)]^+$ at the same excitation wavelength. The variation in $\Phi_{em}$ with excitation wavelength for this complex is shown in Figure 4.

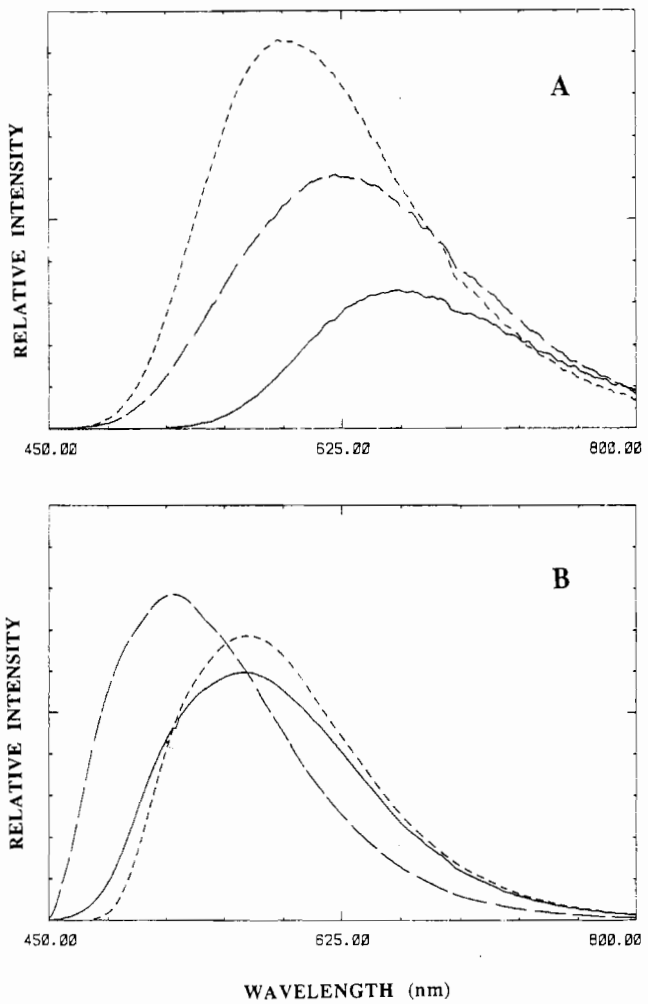


**Figure 5.** (A) Emission spectra at constant absorbance (0.1) in $CH_3CN$ at 293 K for $[(b(CO_2Et)_2)(CO)_3Re^I(3,3'\text{-}(Me)_2\text{-}4,4'\text{-}bpy)Re^I(CO)_3(b)]^{2+}$ (--), $[(b(CO_2Et)_2)(CO)_3Re^I(4\text{-}Etpy)]^+$ (—), and $[(b)(CO)_3Re^I(4\text{-}Etpy)]^+$ (--) at 380-nm excitation. (B) Emission spectra at constant absorbance (0.1 at 293 K) in a 4:1 (v/v) EtOH/MeOH glass at 77 K for $[(b(CO_2Et)_2)(CO)_3Re^I(4,4'\text{-}bpy)Re^I(CO)_3(b(CO_2Et)_2)]^{2+}$ (--), $[(b)(CO)_3Re^I(4,4'\text{-}bpy)Re^I(CO)_3(b)]^{2+}$ (--), and $[(b)(CO)_3Re^I(4,4'\text{-}bpy)Re^I(CO)_3(b(CO_2Et)_2)]^{2+}$ (—) at $\lambda_{exc}$ = 360 nm.

Emission maxima and $\Phi_{em}$ values for the series of complexes in $CH_3CN$, PC, or DCE are collected in Table III.

**Emission Spectra. 77 K.** Emission spectra at 77 K in 4:1 (v/v) EtOH/MeOH glasses for $[(b(CO_2Et)_2)(CO)_3Re^I(4\text{-}Etpy)]^+$, $[(b)(CO)_3Re^I(4\text{-}Etpy)]^+$, $[(b(NH_2)_2)(CO)_3Re^I(4\text{-}Etpy)]^+$,

**Table IV.** Emission Decay Lifetimes at 293 ± 2 K following Excitation at 390 nm[a]

| complex | τ, ns | | | | |
|---|---|---|---|---|---|
| | | | | 4:1 EtOH/MeOH | |
| | $CH_3CN$ | PC | DCE | RT[e] | 77 K |
| $[(b(NH_2)_2)(CO)_3Re(4\text{-Etpy})]^+$ | 940 | | 1420 | 1400 | 14000 |
| $[(b(NH_2)_2)(CO)_3Re(4,4'\text{-bpy})Re(CO)_3(b(NH_2)_2)]^{2+}$ | 64 | 49 | 690 | 89 | *b* |
| $[(b(Me)_2)(CO)_3Re(4,4'\text{-bpy})]^+$ | 341 | 328 | 920 | 345 | |
| $[(b(Me)_2)(CO)_3Re(4,4'\text{-bpy})Re(CO)_3(b(Me)_2)]^{2+}$ | 432 | 335 | 1980 | 595 | |
| $[(b)(CO)_3Re(4\text{-Etpy})]^+$ | 218 | 195 | 505 | 176 | 4550 |
| $[(b)(CO)_3Re(4,4'\text{-bpy})]^+$ | 250 | | | 280 | 4785 |
| $[(b)(CO)_3Re(3,3'\text{-}(Me)_2\text{-}4,4'\text{-bpy})]^+$ | 270 | 230 | 710 | 238 | |
| $[(b)(CO)_3Re(bpa)Re(CO)_3(b)]^{2+}$ | 200 | | 510 | 180 | 4620 |
| $[(b)(CO)_3Re(4,4'\text{-bpy})Re(CO)_3(b)]^{2+}$ | 365 | 325 | 870 | 321 | *b* |
| $[(b(CO_2Et)_2)(CO)_3Re(4\text{-Etpy})]^+$ | 79 | | | 58 | |
| $[(b(CO_2Et)_2)(CO)_3Re(4,4'\text{-bpy})Re(CO)_3(b(CO_2Et)_2)]^{2+}$ | 118 | 100 | 314 | 78 | *b* |
| $[(b(NH_2)_2(CO)_3Re(4,4'\text{-bpy})Re(CO)_3(b)]^{2+}$ | 42 ($a_1$ = 0.34)[c]<br>360 ($a_2$ = 0.30) | | | | |
| $[(b(NH_2)_2)(CO)_3Re(4,4'\text{-bpy})Re(CO)_3(b(CO_2Et)_2)]^{2+}$ | 99 | 80 | 261 | 60 | *b* |
| $[(b(Me)_2)(CO)_3Re(4,4'\text{-bpy})Re(CO)_3(b)]^{2+}$ | 388 | 328 | 1060 | | |
| $[(b)(CO)_3Re(4,4'\text{-bpy})Re(CO)_3(b(CO_2Et)_2]^{2+}$ | 116 | 100 | 340 | 74 | *b* |
| $[(b)(CO)_3Re(3,3'\text{-}(CH_3)_2\text{-}4,4'\text{-bpy})Re(CO)_3(b(CO_2Et)_2)]^{2+}$[d] | 126 ($a_1$ = 1.45)[c]<br>300 ($a_2$ = 0.22) | | *b* | | *b* |

[a] The estimated uncertainties are ±3%. [b] The decays were complex and nonexponential and could not be satisfactorily fit to eq 2. [c] The decay parameters were obtained by fitting the data to eq 2. [d] The bridging ligand is 3,3'-dimethyl-4,4'-bipyridine. [e] RT = room temperature.

$[(b)(CO)_3Re^I(bpa)Re^I(CO)_3(b)]^{2+}$, and $[(b)(CO)_3Re^I(4,4'\text{-bpy})Re^I(CO)_3(b)]^{2+}$ display no excitation wavelength effects. Spectra are shown in Figure 5B for $[(b(CO_2Et)_2)(CO)_3Re^I(4,4'\text{-bpy})Re^I(CO)_3(b(CO_2Et)_2)]^{2+}$, $[(b)(CO)_3Re^I(4,4'\text{-bpy})Re^I(CO)_3(b)]^{2+}$, and $[(b)(CO)_3Re^I(4,4'\text{-bpy})Re^I(CO)_3(b(CO_2Et)_2)]^{2+}$ with 360-nm excitation.

In Figure 6A are shown emission spectra for $[(b(NH_2)_2)(CO)_3Re^I(4\text{-Etpy})]^+$, $[(b(NH_2)_2)(CO)_3Re^I(4,4'\text{-bpy})Re^I(CO)_3(b(NH_2)_2)]^{2+}$ and in Figure 6B for $[(b(NH_2)_2)(CO)_3Re^I(4,4'\text{-bpy})Re^I(CO)_3(b(CO_2Et)_2)]^{2+}$ obtained with excitation at 360 and 400 nm. In the glass, the structured emission for $[(b(NH_2)_2)(CO)_3Re^I(4\text{-Etpy})]^+$ is from a localized $\pi,\pi^*$ state.[16] For both ligand-bridged complexes, excitation at 350 nm leads to relatively low energy emission but with the appearance of a weak $\pi \rightarrow \pi^*$ component at 460 nm. In both cases, the intensity of the $\pi \rightarrow \pi^*$ emission decreases upon excitation at lower energy (390 nm and below). The emission spectra for $[(b(NH_2)_2)(CO)_3Re^I(4,4'\text{-bpy})Re^I(CO)_3(b(NH_2)_2)]^{2+}$ and $[(b(Me)_2)(CO)_3Re^I(4,4'\text{-bpy})Re^I(CO)_3(b(Me)_2)]^{2+}$ are temperature-dependent above the glass-to-fluid transition from 290 to 140 K. The temperature effects are currently under investigation.[17]

**Emission Lifetimes.** Emission decay lifetimes at 295 K in three different solvents are listed in Table IV. The data gave satisfactory fits to single exponential decay kinetics unless otherwise noted. The lifetimes were independent of excitation wavelength (337, 390, or 420 nm) except for $[(b)(CO)_3Re^I(3,3'\text{-}(Me)_2\text{-}4,4'\text{-bpy})Re^I(CO)_3(b(CO_2Et)_2)]^{2+}$. Emission decay from this complex, following 337-, 390-, or 400-nm excitation with monitoring in the region 550–700 nm, could be fit reasonably well to the biexponential function in eq 2 by using the decay parameters listed in Table IV.

When the dimers are compared to the analogous 4-Etpy complexes, there is evidence for bridge-based effects in the ligand-bridged complexes. To summarize, (a) in $[(b(CO_2Et)_2)(CO)_3Re^I(4,4'\text{-bpy})Re^I(CO)_3(b(CO_2Et)_2)]^{2+}$, the emitting state is $(b(CO_2Et)_2)$ localized and a 25% enhancement of the lifetime is observed compared to $[(b(CO_2Et)_2)(CO)_3Re^I(4\text{-Etpy})]^+$; (b) in $[(b(NH_2)_2)(CO)_3Re^I(4,4'\text{-bpy})Re^I(CO)_3(b(NH_2)_2)]^{2+}$, emission occurs from the bridged-based MLCT state (vide infra) and the lifetime is shortened considerably; and (c) in $[(b)(CO)_3Re^I(4,4'\text{-bpy})Re^I(CO)_3(b)]^{2+}$, bridge-localized and bpy-localized MLCT excited states are in equilibrium. The emission lifetime is enhanced by 75% compared to $[(b)(CO)_3Re^I(4\text{-Etpy})]^+$.[17] From the emission data in Table IV, solvent dependences are observed

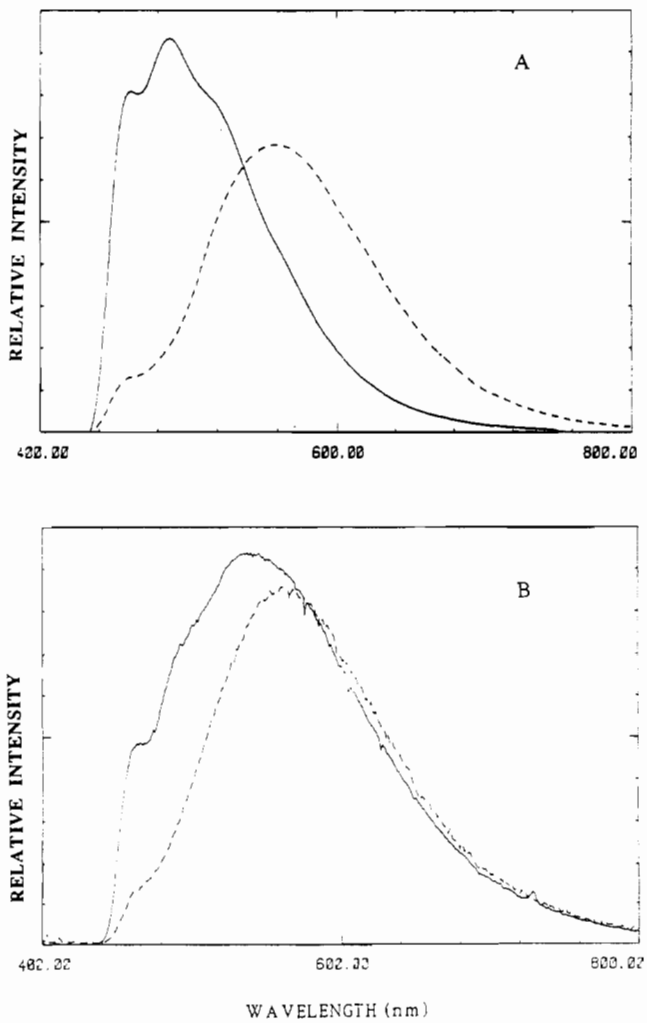


**Figure 6.** Emission spectra at constant absorbance (0.1 at 293 K) in a 4:1 (v/v) EtOH/MeOH glass at 77 K for (A) $[(b(NH_2)_2)(CO)_3Re^I(4\text{-Etpy})]^+$ (—) at $\lambda_{exc}$ = 350 nm and $[(b(NH_2)_2)(CO)_3Re^I(4,4'\text{-bpy})Re^I(CO)_3(b(CO_2Et)_2)]^{2+}$ (--) at $\lambda_{exc}$ = 360 nm and (B) $[(b(NH_2)_2)(CO)_3Re^I(4,4'\text{-bpy})Re^I(CO)_3(b(NH_2)_2)]^{2+}$ at $\lambda_{exc}$ = 360 nm (—) and at $\lambda_{exc}$ = 400 nm (--).

(16) Worl, L.; Della Ciana, L.; Duesing, R.; Meyer, T. J. Manuscript in preparation.
(17) Tapolsky, G.; Duesing, R.; Meyer, T. J. Submitted for publication.
(18) Curtis, J. C.; Bernstein, J. S.; Meyer, T. J. *Inorg. Chem.* **1985**, *24*, 385.

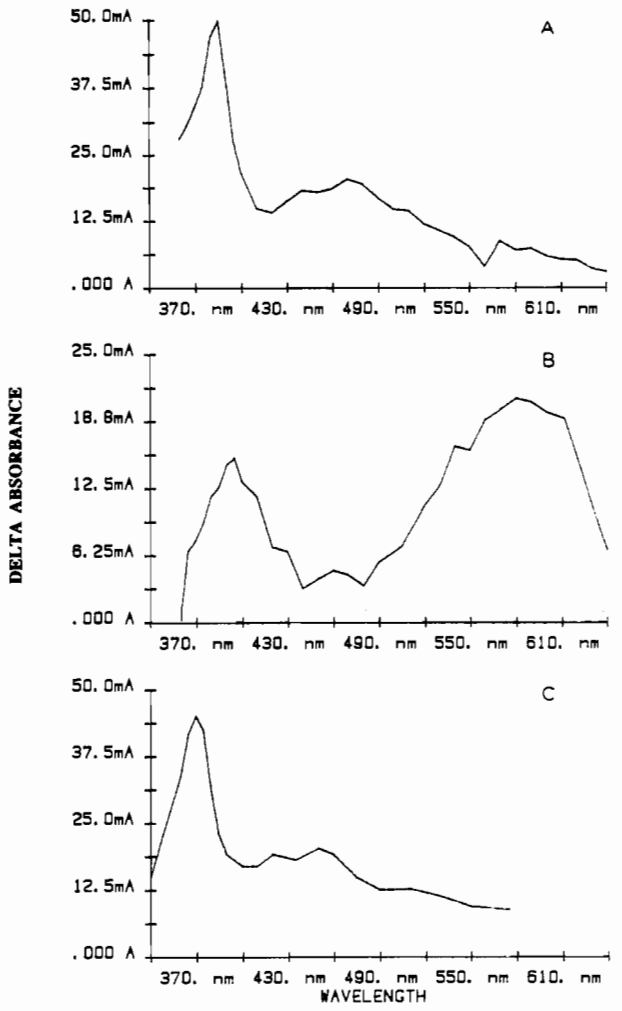


**Figure 7.** Transient absorbance difference spectra obtained 50 ns after the laser pulse in freeze–pump–thaw deoxygenated acetonitrile solutions at 293 ± 2 K for (A) $[(b(CO_2Et)_2)(CO)_3Re^I(4,4'\text{-bpy})Re^I(CO)_3(b\text{-}(CO_2Et)_2)]^{2+}$, (B) $[(b(Me)_2)(CO)_3Re^I(4,4'\text{-bpy})Re^I(CO)_3(b(Me)_2)]^{2+}$, and (C) $[(b(Me)_2)(CO)_3Re^I(4,4'\text{-bpy})]^+$. The ground-state absorbance was ~0.7 at the excitation wavelength, 355 nm. The laser pulse energy was 4 mJ/pulse.

in all cases but are especially dramatic for $[(b(NH_2)_2)\text{-}(CO)_3Re^I(4,4'\text{-bpy})Re^I(CO)_3(b(NH_2)_2)]^{2+}$.

Emission decays in 4:1 (v/v) ethanol/methanol glasses at 77 K are reasonably exponential for $[(b(NH_2)_2)(CO)_3Re^I(4\text{-Etpy})]^+$, $[(b)(CO)_3Re^I(4\text{-Etpy})]^+$, $[(b(CO_2Et)_2)(CO)_3Re^I(4\text{-Etpy})]^+$, and the bpa-bridged complex. For the 4,4′-bpy-bridged complexes, the emission decay kinetics are sufficiently complex that the data could not be fit to the biexponential expression in eq 2. Both time and excitation wavelength effects are observed in the low-temperature spectrum of $[(b(NH_2)_2)(CO)_3Re^I(4,4'\text{-bpy})Re^I(CO)_3\text{-}(b(NH_2)_2)]^{2+}$. For example, following 390-nm excitation, emission monitored at 710 nm shows an initial emission intensity that *increases* reaching a maximum at ~60 ns followed by the decay of the signal.

**Transient Absorbance.** Transient absorbance difference spectra for $[(b(CO_2Et)_2)(CO)_3Re^I(4,4'\text{-bpy})Re^I(CO)_3(b(CO_2Et)_2)]^{2+}$, $[(b(Me)_2)(CO)_3Re^I(4,4'\text{-bpy})Re^I(CO)_3(b(Me)_2)]^{2+}$, and $[(b\text{-}(Me)_2)(CO)_3Re^I(4,4'\text{-bpy})]^{2+}$ in $CH_3CN$ at room temperature are shown in Figure 7. The spectra were acquired 50 ns after laser excitation at 355 nm in $CH_3CN$. For $[(b(CO_2Et)_2)\text{-}(CO)_3Re^I(4,4'\text{-bpy})Re^I(CO)_3(b(CO_2Et)_2)]^{2+}$ or $[(b(Me)_2)\text{-}(CO)_3Re^I(4,4'\text{-bpy})]^+$, intense absorption features appear at 380–385 or 365–370 nm, respectively. For $[(b(Me)_2)\text{-}(CO)_3Re^I(4,4'\text{-bpy})Re^I(CO)_3(b(Me)_2)]^{2+}$, absorption features appear at 390–400 and 570–600 nm. When compared to the spectra of related $MQ^+$ complexes such as $[(b)(CO)_3Re^I\text{-}(MQ^+)]^{2+}$, ($MQ^+$ is the *N*-methyl-4,4′-bipyridinium cation), the

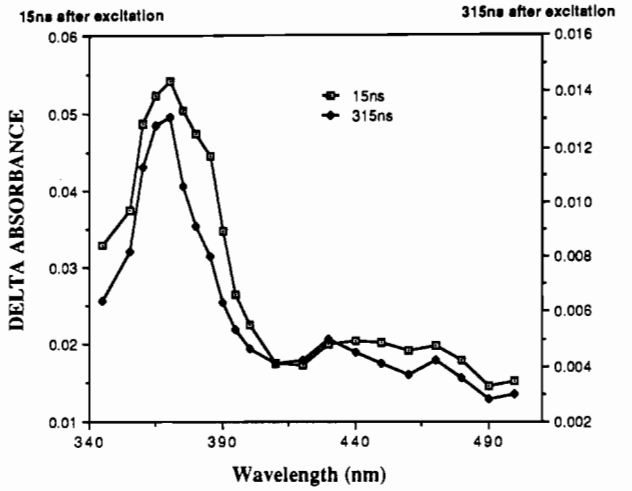


**Figure 8.** Transient absorbance difference spectra obtained in freeze–pump–thaw deoxygenated acetonitrile solutions at 293 ± 2 K for $[(b)\text{-}(CO)_3Re^I(3,3'\text{-}(Me)_2\text{-}4,4'\text{-bpy})Re^I(CO)_3(b(CO_2Et)_2)]^{2+}$ 15 ns (left scale) and 315 ns (right scale) after the laser pulse. The ground-state absorbance was ~0.7 at the excitation wavelength, 355 nm, and the laser pulse energy was 4mJ/pulse.

low-energy absorption feature in the ligand-bridged complexes presumably arises from $\pi^* \rightarrow \pi^*$ transitions at the singly reduced 4,4′-bpy bridging ligand.[6,19,20] In this excited state, the two pyridyl rings presumably adopt a coplanar orientation.[20–23]

The transient absorbance difference spectra of $[(b(NH_2)_2)\text{-}(CO)_3Re^I(4,4'\text{-bpy})Re^I(CO)_3(b(NH_2)_2)]^{2+}$,[11] $[(b(NH_2)_2)\text{-}(CO)_3Re^I(4,4'\text{-bpy})Re^I(CO)_3(b)]^{2+}$, and $[(b(Me)_2)(CO)_3Re^I\text{-}(4,4'\text{-bpy})Re^I(CO)_3(b)]^{2+}$ also show the intense absorption feature at 570–600 nm characteristic of a 4,4′-bpy-localized MLCT excited state. For $[(b)(CO)_3Re^I(4,4'\text{-bpy})Re^I(CO)_3(b)]^{2+}$, absorption features for *both* $Re^{II}(bpy^{\bullet-})$ and $Re^{II}(4,4'\text{-}bpy^{\bullet-})$ excited states can be seen in transient absorbance difference spectra in polar solvents such as propylene carbonate.[17] For $[(b(NH_2)_2)\text{-}(CO)_3Re^I(4,4'\text{-bpy})Re^I(CO)_3(b(CO_2Et)_2)]^{2+}$ and $[(b)\text{-}(CO)_3Re^I(4,4'\text{-bpy})Re^I(CO)_3(b(CO_2Et)_2)]^{2+}$ the characteristic $\pi \rightarrow \pi^*(b^{\bullet-}(CO_2Et)_2)$ absorption feature appears at $\lambda_{max} \simeq$ 380–385 nm.

In Figure 8 are shown transient absorbance difference spectra in $CH_3CN$ for $[(b)(CO)_3Re^I(3,3'\text{-}(Me)_2\text{-}4,4'\text{-bpy})Re^I(CO)_3(b\text{-}(CO_2Et)_2)]^{2+}$ acquired 15 and 315 ns after laser excitation. The spectrum is time-dependent with the loss of the low-energy $\pi \rightarrow \pi^*(b^{\bullet-}(CO_2Et)_2)$ shoulder in the broad absorption feature at 360–390 nm occurring more rapidly than the $\pi \rightarrow \pi^*(b^{\bullet-})$ band due to the differences in their excited-state lifetimes (120 vs 260 ns). The change in the spectrum is nearly complete after 315 ns. It is followed by the slower, general loss of absorbance with time for the $\pi \rightarrow \pi^*(b^{\bullet-})$ absorption feature.

In a separate experiment, a transient absorbance difference spectrum was obtained for a solution ~$1 \times 10^{-4}$ M in both $[(b)(CO)_3Re^I(4\text{-Etpy})]^+$ and $[(b(CO_2Et)_2)(CO)_3Re^I(4\text{-Etpy})]^+$ following excitation at 355 nm. The spectrum was superimposable

(19) (a) Chen, P.; Danielson, E.; Meyer, T. J. *J. Phys. Chem.* **1988**, *92*, 3708. (b) Kosower, E. M.; Cotter, J. L. *J. Am. Chem. Soc.* **1964**, *86*, 5524. (c) Wanatabe, T.; Honda, K. *J. Phys. Chem.* **1982**, *86*, 2617. (d) Chen, P.; Wesmoreland, T. D.; Danielson, E.; Schanze, K. S.; Anthon, D.; Neveux, P. E., Jr.; Meyer, T. J. *Inorg. Chem.* **1987**, *26*, 116.
(20) Chen, P.; Curry, M.; Meyer, T. J. *Inorg. Chem.* **1989**, *28*, 2272.
(21) (a) Kubel, F.; Strohle, J. *Z. Naturforsch., B. Anorg. Chem., Org. Chem.* **1982**, *B37*, 272. (b) Julve, M.; Verdaguer, M.; Faus, J.; Tinti, F.; Moratal, J.; Monge, A.; Gutierrez-Puebla, E. *Inorg. Chem.* **1987**, *26*, 3520.
(22) (a) Inamura, A.; Hoffmann, R. *J. Am. Chem. Soc.* **1968**, *90*, 5379. (b) Momicchioli, M.; Bruni, M. C.; Baraldi, I. *J. Phys. Chem.* **1972**, *76*, 3983. (c) Takahashi, C.; Maeda, S. *Chem. Phys. Lett.* **1974**, *24*, 584. (d) Yamaguchi, S.; Yashimizu, N.; Maeda, S. *J. Phys. Chem.* **1978**, *82*, 1078.
(23) (a) Cooke, B. J.; Palmer, T. F. *J. Photochem.* **1984**, *26*, 149. (b) Naqvi, K. R.; Donatsch, J.; Wilder, U. P. *Chem. Phys. Lett.* **1975**, *34*, 285. (c) Fujii, T.; Suzuki, S.; Komatsu, S. *Chem. Phys. Lett.* **1978**, *57*, 175.

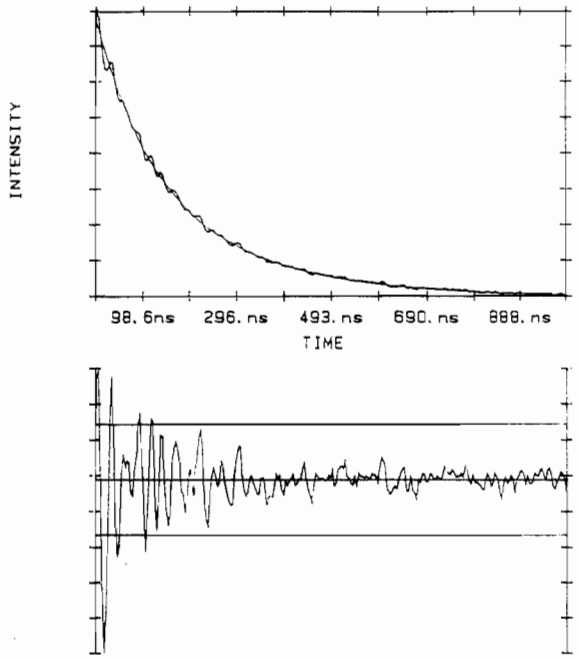


**Figure 9.** Transient absorbance decay curve for $[(b)(CO)_3Re^I(3,3'\text{-}(Me)_2\text{-}4,4'\text{-}bpy)Re^I(CO)_3(b(CO_2Et)_2)]^{2+}$ in freeze–pump–thaw deoxygenated acetonitrile solution at 293 ± 2 K. The excitation wavelength was 355 nm, and the transient absorbance signal was monitored at 380 nm. Intensity vs time and residual plots, calculated by using eq 2 and the kinetic parameters in Table IV, are also shown.

in profile, maximum, and relative intensities with the spectrum of $[(b)(CO)_3Re^I(3,3'\text{-}(Me)_2\text{-}4,4'\text{-}bpy)Re^I(CO)_3(b(CO_2Et)_2)]^{2+*}$. The ratio of absorbances at 365–375 to 380–390 nm was, within experimental error, the same for the two solutions (1.24 and 1.28). These results show that the same relative amounts of the $Re^{II}(bpy^{\bullet-})$ and $Re^{II}(b^{\bullet-}(CO_2Et)_2)$ excited states are formed in the ligand-bridged complex as in the separated complexes following excitation at 355 nm. It follows from these results that intramolecular energy transfer in the ligand-bridged complex must be slow on the time scale for decay of the $Re^{II}(b^{\bullet-})$ excited state (~220 ns).

A transient absorbance-time decay curve for $[(b)(CO)_3Re^I(3,3'\text{-}(Me)_2\text{-}4,4'\text{-}bpy)Re^I(CO)_3(b(CO_2Et)_2)]^{2+}$ following 355-nm excitation is shown in Figure 9. The fit of the data to the biexponential function in eq 2 by using the kinetic parameters in Table IV is also shown. Excitation at 420 nm leads to a shift in the transient absorbance maximum to 385 nm. Transient absorbance decay following 420-nm excitation can be fit to a single exponential with $\tau = 115 \pm 10$ ns. Ground-state absorbance at 420 nm is dominated by the $d\pi(Re) \rightarrow \pi^*(b(CO_2Et)_2)$ transition, Figure 2B. Excited-state decay determinations by transient emission or absorbance measurements gave the same results within experimental error.

In order to investigate the influence of distance and electronic coupling between the two metal sites on photophysical properties, the complexes $[(b)(CO)_3Re^I(pyrazine)Re^I(CO)_3(b)]^{2+}$ and $[(b)(CO)_3Re^I(1,2\text{-dipyridylethylene})Re^I(CO)_3(b)]^{2+}$ were also prepared. The pyrazine-bridged complex was labile toward solvolysis, and its photophysical properties could not be studied. In the complex with 1,2-dipyridylethylene as the bridging ligand, following MLCT $d\pi(Re) \rightarrow \pi^*(b)$ excitation, nearly complete quenching of the MLCT emission occurs at all temperatures from 298 to 100 K in 4:1 (v/v) ethanol/methanol. We presume that the origin of the quenching is via intramolecular sensitization of a $\pi\pi^*$ state transition largely localized on the olefin portion of the bridging ligand.

## Discussion

**Control of the Electron Acceptor Site by Substituent Changes at bpy.** The electrochemical measurements show that the electron-withdrawing $CO_2Et$ substituents lower $\pi^*(b(CO_2Et)_2)$ by ~0.4 V relative to $\pi^*(4,4'\text{-bpy})$. Accordingly, MLCT excitation of $[(b(CO_2Et)_2)(CO)_3Re^I(4,4'\text{-bpy})Re^I(CO)_3(b(CO_2Et)_2)]^{2+}$ leads to a $Re^{II}(b^{\bullet-}(CO_2Et)_2)$ localized excited state as shown by the transient absorption and emission results. By contrast, in the complexes $[(b(X)_2)(CO)_3Re^I(4,4'\text{-bpy})Re^I(CO)_3(b(X)_2)]^{2+}$ with the electron-donating substituents $CH_3$ or $NH_2$, $\pi^*(b(X)_2)$ is increased relative to $\pi^*(4,4'\text{-bpy})$ by ~0.25 and ~0.5 V, respectively. Excitation of either leads to the low-energy absorption feature at 570–600 nm, which is characteristic of electronic occupation of a $\pi^*$ level delocalized over the 4,4'-bpy bridging ligand. For $[(b(NH_2)_2)(CO)_3Re^I(4,4'\text{-bpy})Re^I(CO)_3(b(NH_2)_2)]^{2+}$, a weak, red-shifted emission from the $Re^{II}(4,4'\text{-}(bpy^{\bullet-}))$ state is observed.

**Chart I.** Relative Energies of the $4,4'\text{-}(X)_2$-bpy- and 2,2'-bpy-Based MLCT Excited States

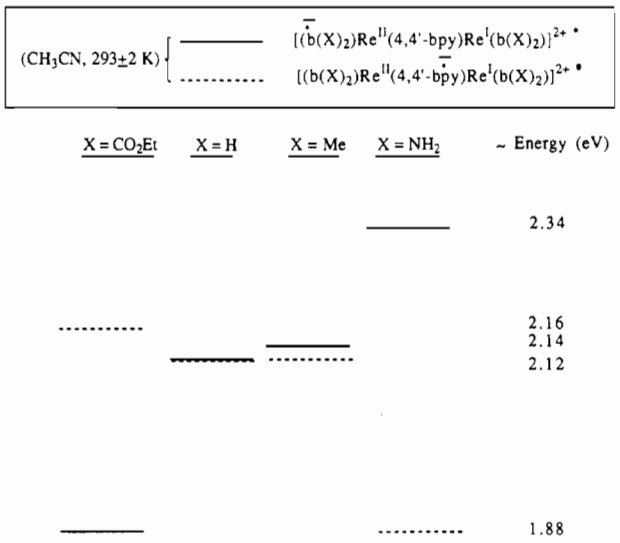


The effects of substituent changes at 2,2'-bpy on the relative energies of the $\pi^*(b(X)_2)$- and $\pi^*(4,4'\text{-bpy})$-based MLCT states are illustrated in Chart I. The $\pi^*(b(X)_2)$-based states are indicated by a solid line and the $\pi^*(4,4'\text{-bpy})$-based states by a dashed line. The energies of the $\pi^*(b(X)_2)$-based states were taken as actual emission energies for X = $CO_2Et$ or H and as emission energies for the related 4-Etpy complexes for X = $NH_2$ or $Me_2$. The energy of the 4,4'-bpy-based excited state in $[(b\text{-}(CO_2Et)_2)(CO)_3Re^I(4,4'\text{-bpy})Re^I(CO)_3(b(CO_2Et)_2)]^{2+}$ was calculated from the difference in absorbance maxima between the $d\pi(Re) \rightarrow \pi^*(b(CO_2Et)_2)$ and $d\pi(Re) \rightarrow \pi^*(4,4'\text{-bpy})$ transitions in Figure 1.

The presentation in Chart I provides a qualitative basis for explaining the origin of the substituent effects. The effect of substituent changes on the energies of the $Re^{II}(b^{\bullet-}(X)_2)$ states is direct since they influence the energy of the $\pi^*$ acceptor level. Variation from electron-donating ($NH_2$) to electron-withdrawing ($CO_2Et$) substituents decreases the energy of the $Re^{II}(b^{\bullet-})\text{-}(X)_2$-based states by ~0.5 eV.

The effect of substituent changes on the $Re^{II}(4,4'\text{-}(bpy^{\bullet-}))$-based excited states is indirect since the $\pi^*$ acceptor level is on 4,4'-bpy. These substituent effects are transmitted indirectly via $\pi,\pi^*(b(X)_2)$ to the $d\pi$ orbitals of Re(I). Because of the indirect nature of the interaction, the $\pi^*(4,4'\text{-bpy})$ levels are *stabilized* by electron-donating groups and *destabilized* by electron-withdrawing groups. The variation from X = $NH_2$ to X = $CO_2Et$ leads to an *increase* in the energy of the $Re^{II}(4,4'\text{-}bpy^{\bullet-})$ excited state of ~0.26 eV.

Because of their opposite effects on $Re^{II}(4,4'\text{-}bpy^{\bullet-})$ and $Re^{II}(b^{\bullet-}(X)_2)$, substituent changes can be utilized to control the final electron acceptor site and, with it, the relative ordering of excited states. With X = $CO_2Et$, the lowest excited state is bpy based; with X = $NH_2$ or $CH_3$, it is 4,4'-bpy based. With X = H, a balance is reached and both states are in a solvent-dependent equilibrium.[17]

**Excited-State Dynamics.** For all of the 4,4'-bpy-bridged complexes, excited-state decay at room temperature is excitation

wavelength independent and follows first-order kinetics. The absence of excitation effects in regions where more than one chromophore absorbs shows that the intramolecular electron-transfer processes by which higher states reach the lowest must be rapid ($\tau < 10$ ns). An example is shown below.

$$\xrightarrow{h\nu} [(b^{\bullet-}(NH_2)_2)(CO)_3\text{-}Re^{II}(4,4'\text{-bpy})Re^{I}(CO)_3(b(NH_2)_2)]^{2+*} \rightarrow [(b(NH_2)_2)(CO)_3Re^{II}(4,4'\text{-bpy}^{\bullet-})Re^{I}(CO)_3(b(NH_2)_2)]^{2+*}$$

Intramolecular electron transfer continues to occur at 77 K in a 4:1 (v/v) ethanol/methanol glass in some cases, but there is evidence for excitation effects. A small residual $\pi\pi^*(b(NH_2)_2)$ emission appears for $[(b(NH_2)_2)(CO)_3Re^{I}(4,4'\text{-bpy})Re^{I}(CO)_3(b(NH_2)_2)]^{2+}$. In $[(b)(CO)_3Re^{I}(4,4'\text{-bpy})Re^{I}(CO)_3(b(CO_2Et)_2)]^{2+}$, $d\pi(Re) \rightarrow \pi^*(b)$ and $d\pi(Re) \rightarrow \pi^*(4,4'\text{-bpy})$ excitation at 360 nm leads to a small amount of residual emission from the $Re^{II}(b^{\bullet-})$-based state.

These observations suggest that, at 77 K, the time scale for $b^{\bullet-}(NH_2) \rightarrow 4,4'\text{-bpy}$ or $b^{\bullet-} \rightarrow 4,4'\text{-bpy}$ intramolecular electron transfer is comparable to the decay times for the lowest energy state. The resulting kinetic complications would explain the nonexponential decays at 77 K. Matrix effects may also play a role.[24,25] However, excited-state decay in $[(b)(CO)_3Re^{I}(bpa)Re^{I}(CO)_3(b)]^{2+}$ or in $[(b)(CO)_3Re^{I}(4\text{-Etpy})]^{+}$ is reasonably exponential. This suggests that the nonexponential behavior in the 4,4'-bpy-bridged complexes is dominated by competing dynamical intramolecular processes. For $[(b)(CO)_3Re^{I}(4,4'\text{-bpy})Re^{I}(CO)_3(b)]^{2+*}$, it has been concluded that intramolecular electron transfer is slow at 77 K.[17]

**Intramolecular Energy Transfer.** In $[(b(NH_2)_2)(CO)_3Re^{I}(4,4'\text{-bpy})Re^{I}(CO)_3(b(CO_2Et)_2)]^{2+}$ or $[(b)(CO)_3Re^{I}(4,4'\text{-bpy})Re^{I}(CO)_3(b(CO_2Et)_2)]^{2+}$, the differences in energy between the higher and lower energy $Re^{II}(b^{\bullet-}(X)_2)$-based MLCT states across the bridge are ~0.45 and ~0.25 eV, respectively. At room temperature, excitation at the higher energy chromophore is followed by rapid, quantitative intramolecular energy transfer. This is shown by (1) the appearance of the $Re^{II}(b^{\bullet-}(CO_2Et)_2)$-based emission independent of excitation wavelength; (2) the transient absorbance feature at 385 nm, which is characteristic of a $(b^{\bullet-}(CO_2Et)_2)$-based excited state; and (3) the absence of the low-energy absorption feature characteristic of $Re^{II}(4,4'\text{-bpy}^{\bullet-})$ in the transient absorbance difference spectrum.

Ground-state absorption spectra from 330 to 420 nm are a badly convoluted mix of $d\pi(Re) \rightarrow \pi^*(b(X)_2)$ and $d\pi(Re) \rightarrow \pi^*(4,4'\text{-bpy})$ transitions. Excitation in this region leads to the $Re^{II}(b^{\bullet-}(CO_2Et)_2)$-based state by direct excitation. In addition, either $d\pi(Re) \rightarrow \pi^*(4,4'\text{-bpy})$ or $d\pi(Re) \rightarrow \pi^*(b)$ excitation leads to the final $Re^{II}(b^{\bullet-}(CO_2Et)_2)$ state on a time scale that is short compared to its decay time (115 ns). This is shown by the excitation wavelength independent (337–420-nm) single-exponential decay kinetics.

From these observations, either $d\pi(Re) \rightarrow \pi^*(bpy)$ or $d\pi(Re) \rightarrow \pi^*(4,4'\text{-bpy})$ excitation in $[(b)(CO)_3Re^{I}(4,4'\text{-bpy})Re^{I}(CO)_3(b(CO_2Et)_2)]^{2+}$ is followed by rapid ($k > 2 \times 10^8$ s$^{-1}$) intramolecular energy transfer at room temperature.

$$\xrightarrow{h\nu} [b^{\bullet-}(CO)_3Re^{II}(4,4'\text{-bpy})Re^{I}(CO)_3(b(CO_2Et)_2)]^{2+*} \rightarrow [(b)(CO)_3Re^{I}(4,4'\text{-bpy})Re^{II}(CO)_3(b^{\bullet-}(CO_2Et)_2)]^{2+*}$$

$$\xrightarrow{h\nu} [(b)(CO)_3Re^{II}(4,4'\text{-bpy}^{\bullet-})Re^{I}(CO)_3(b(CO_2Et)_2)]^{2+*} \rightarrow [(b)(CO)_3Re^{I}(4,4'\text{-bpy})Re^{II}(CO)_3(b^{\bullet-}(CO_2Et)_2)]^{2+*}$$

The comparison between $[(b(CO_2Et)_2)(CO)_3Re^{I}(4,4'\text{-bpy})Re^{I}(CO)_3(b(CO_2Et)_2)]^{2+}$ and $[(b)(CO)_3Re^{I}(4,4'\text{-bpy})Re^{I}(CO)_3(b(CO_2Et)_2)]^{2+}$ in Figure 4 suggests that the quantum yield for intramolecular energy transfer in the unsymmetrical complex must be nearly unity. The decrease in quantum yield of ca. 15% at high energy over the wavelength range 350–420 nm for these complexes and for $[(b(CO_2Et)_2)(CO)_3Re^{I}(4,4'\text{-bpy})Re^{I}(CO)_3(b(CO_2Et)_2)]^{2+}$ is not understood. In may arise from inefficient internal conversion between $\pi\pi^*(b;b(X)_2)$ and MLCT excited states. The spectra are increasingly convoluted with the $\pi \rightarrow \pi^*$ transitions at higher energies.

Comparisons between $[(b)(CO)_3Re^{I}(3,3'\text{-}(Me)_2\text{-}4,4'\text{-bpy})Re^{I}(CO)_3(b(CO_2Et)_2)]^{2+}$ and $[(b)(CO)_3Re^{I}(4,4'\text{-bpy})Re^{I}(CO)_3(b(CO_2Et)_2)]^{2+}$ show that the rate of $Re^{II}(b^{\bullet-}) \rightarrow Re^{II}(b^{\bullet-}(CO_2Et)_2)$ intramolecular energy transfer is highly dependent upon the ligand bridge. For 3,3'-$(Me)_2$-4,4'-bpy as the bridge, contributions appear in transient absorbance and emission spectra from both the $Re^{II}(b^{\bullet-})$ and $Re^{II}(b^{\bullet-}(CO_2Et)_2)$ excited states.[11] The rates of decay of the two states seem to be largely uncoupled and the rate of intramolecular energy transfer slow. The observations that lead to this conclusion are as follows. (1) The initial loss in absorbance at 385 nm in the time-dependent transient spectrum in Figure 8 shows that the $Re^{II}(b^{\bullet-}(CO_2Et)_2)$ state decays more rapidly than the $Re^{II}(b^{\bullet-})$ state. After 315 ns, only the higher energy $Re^{II}(b^{\bullet-})$ state with $\lambda_{max} = 370$ nm is present in significant amounts. (2) The emission spectrum of the dimeric complex in Figure 5A is a superposition of the spectra of $[(b)(CO)_3Re^{I}(4\text{-Etpy})]^{+}$ and $[(b(CO_2Et)_2)(CO)_3Re^{I}(4\text{-Etpy})]^{+}$ and shows the excitation wavelength dependence expected for isolated chromophores. (3) The contrast in the wavelength-dependent behavior of $\Phi_{em}$ with the other complexes in Figure 4 is expected if the Re(b) and $Re(b(CO_2Et)_2)$ chromophores are uncoupled. The $Re^{II}(b^{\bullet-}(CO_2Et)_2)$ excited state, which is reached by low-energy excitation, is a weaker emitter in $[(b(CO_2Et)_2)(CO)_3Re^{I}(4\text{-Etpy})]^{+}$ ($\Phi_{em} = 0.007$) than the $Re^{II}(b^{\bullet-})$ excited state in $[(b)(CO)_3Re^{I}(4\text{-Etpy})]^{+}$ ($\Phi_{em} = 0.027$). (4) Excitation of a solution ~$1 \times 10^{-4}$ M in both $[(b)(CO)_3Re^{I}(4Etpy)]^{+}$ and $[(b(CO_2Et)_2)(CO)_3Re^{I}(4\text{-Etpy})]^{+}$ gave a ratio of $\pi \rightarrow \pi^*(b^{\bullet-})$ absorptivity at 370 nm to $\pi \rightarrow \pi^*(b^{\bullet-}(CO_2Et)_2)$ absorptivity at 385 nm of 1.24. A ratio of 1.28 was found for $[(b)(CO)_3Re^{I}(3,3'\text{-}(Me)_2\text{-}4,4'\text{-bpy})Re^{I}(CO)_3(b(CO_2Et)_2)]^{2+}$ under the same conditions. The $Re^{II}(b^{\bullet-})$- and $Re^{II}(b^{\bullet-}(CO_2Et)_2)$-based states are formed in the expected amounts based on their relative ground-state absorbances at 355 nm. (5) Excited-state decay in $[(b)(CO)_3Re^{I}(3,3'\text{-}(Me)_2\text{-}4,4'\text{-bpy})Re^{I}(CO)_3(b(CO_2Et)_2)]^{2+*}$ can be fit to biexponential kinetics with characteristic decay constants (120 and 260 ns), which are near those of $[(b)(CO)_3Re^{I}(3,3'\text{-}(Me)_2\text{-}4,4'\text{-bpy})]^{+*}$ and $[(b(CO_2Et)_2)(CO)_3Re^{I}(4\text{-Etpy})]^{+*}$ (Table IV).

Although there may be a contribution in the decay kinetics from direct energy transfer between $Re^{II}(b^{\bullet-})$ and $Re^{II}(b^{\bullet-})(CO_2Et)_2)$ in the 3,3'-$(Me)_2$-4,4'-bpy-bridged complex, it must be relatively insignificant. We estimate from our experimental observations that $k_{et} < 4 \times 10^6$ s$^{-1}$ for direct intramolecular energy transfer.[26]

**Mechanisms of Intramolecular Energy Transfer.** From our observations, the rate of intramolecular $Re^{II}(b^{\bullet-}) \rightarrow Re^{II}(b^{\bullet-}(CO_2Et)_2)$ energy transfer is strongly dependent upon the bridging ligand. With 4,4'-bpy as the bridge, $k_{et} > 2 \times 10^8$ s$^{-1}$. For 3,3'-$(Me)_2$-4,4'-bpy as the bridge, $k_{et} < 4 \times 10^6$ s$^{-1}$. One interpretation of the bridging-ligand effect is that electronic coupling between the Re sites is significantly interrupted with 3,3'-$(Me)_2$-4,4'-bpy as the bridge, which greatly decreases the exchange interactions that promote energy transfer.[1a,27] The steric effects of the methyl groups at the 3 and 3' positions prevent the two rings from assuming a coplanar structure, although the ligand $\pi$ system can support electronic interactions at all interplanar angles except 90°.[14a,20,28]

(24) (a) McGuire, M.; McLendon, G. *J. Phys. Chem.* **1986**, *90*, 2449. (b) Dellinger, B.; Kasha, M. *Chem. Phys. Lett.* **1976**, *38*, 9. (c) Worl, L. A.; Meyer, T. J. *Chem. Phys. Lett.* **1988**, *143*, 541. (d) Lumpkin, R. S.; Meyer, T. J. *J. Phys. Chem.* **1986**, *90*, 5307.

(25) (a) Kakitani, T.; Natago, N. *J. Phys. Chem.* **1988**, *92*, 5059. (b) Shi, W.; Wolfgang, S.; Strekas, T. C.; Gafney, H. D. *J. Phys. Chem.* **1985**, *89*, 974.

(26) The rate constant for intramolecular energy transfer is slower than that for excited-state decay. For the $Re^{II}(b^{\bullet-})$ MLCT state, $\tau \sim 250$ ns, which gives $k < 4 \times 10^6$ s$^{-1}$.

(27) Tanner, M.; Ludi, A. *Inorg. Chem.* **1981**, *20*, 2348.

**Scheme I**

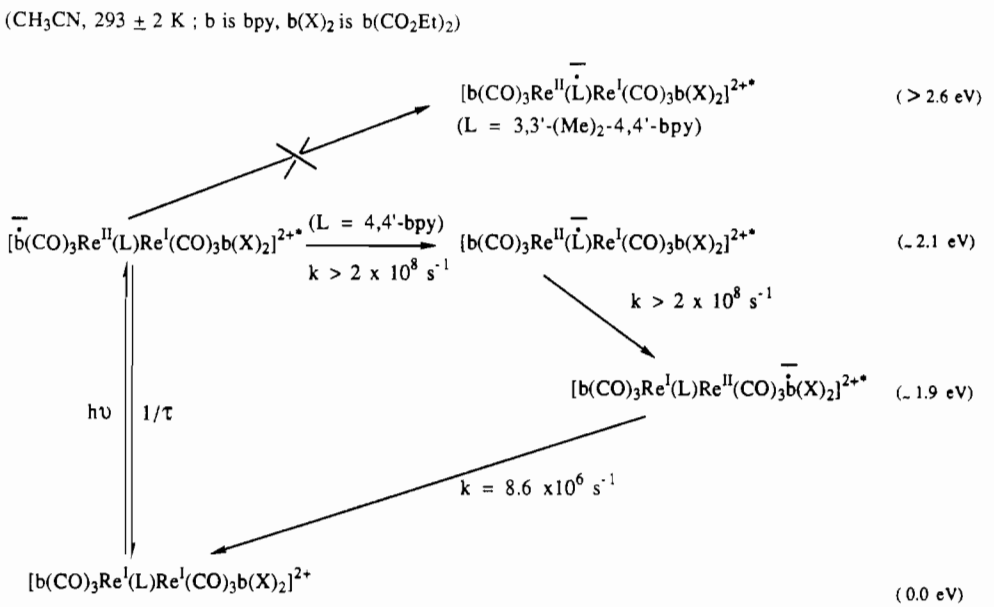


The different electron acceptor characteristics of the two bridging ligands and a mechanism involving initial electron transfer may provide a better explanation. From the electrochemical results in Table I, reduction at the bridge in $[(b)(CO)_3Re^I(4,4'\text{-bpy})Re^I(CO)_3(b(CO_2Et)_2)]^{2+}$ occurs at $\sim -1.2$ V and in $[(b)(CO)_3Re^I(3,3'\text{-}(Me)_2\text{-}4,4'\text{-bpy})Re^I(CO)_3(b(CO_2Et)_2)]^{2+}$ at $<-1.6$ V. The more positive potential for 4,4'-bpy as the acceptor ligand follows from its ability to bring the pyridyl rings to coplanarity. Full occupation of $\pi^*$(4,4'-bpy) leads to a coplanar ring structure in which electron delocalization of the added electron is maximized.[20,29,30]

An electron-transfer mechanism that leads to energy transfer is shown in Scheme I. Following $d\pi(Re) \rightarrow \pi^*(b)$ MLCT excitation, the first step is a $b^{\bullet-} \rightarrow$ 4,4'-bpy electron transfer. This reaction occurs with $\Delta G \sim 0$ for 4,4'-bpy as the bridging ligand but is inaccessible for 3,3'-$(Me)_2$-4,4'-bpy as the bridging ligand where $\Delta G \geq +0.5$ eV. Electron transfer to the bridge is known to be rapid for $[(b)(CO)_3Re^I(4,4'\text{-bpy})Re^I(CO)_3(b)]^{2+*}$. From the results of transient absorbance and emission measurements, $Re^{II}(b^{\bullet-}) \rightarrow Re^{II}(4,4'\text{-bpy}^{\bullet-})$ electron transfer occurs with $k(293 \pm 2$ K, $CH_3CH) > 2 \times 10^8$ $s^{-1}$.[17]

Following electron transfer to the bridge, completion of the overall energy-transfer process could involve any one of three different mechanisms, none of which can be distinguished from the experimental results.

**Mechanism 1.** In mechanism 1, direct $Re^{II}(4,4'\text{-bpy}^{\bullet-}) \rightarrow Re^{II}(b^{\bullet-}(CO_2Et)_2)$ energy transfer occurs, eq 3.

$$[(b)(CO)_3Re^{II}(4,4'\text{-bpy}^{\bullet-})Re^I(CO)_3(b(CO_2Et)_2)]^{2+*} \rightarrow [(b)(CO)_3Re^I(4,4'\text{-bpy})Re^{II}(CO)_3(b^{\bullet-}(CO_2Et)_2)]^{2+*} \quad (3)$$

There are two additional mechanisms that involve sequential electron transfers.

**Mechanism 2.** The initial $d\pi(Re) \rightarrow \pi^*(b)$ excitation creates an excited-state mixed-valence complex, $[(b^{\bullet-})(CO)_3Re^{II}(4,4'\text{-bpy})Re^I(CO)_3(b(CO_2Et)_2)]^{2+*}$.[6] Subsequent $b^{\bullet-} \rightarrow$ 4,4'-bpy electron transfer creates an isomer in which the excited electron resides on the ligand bridge, Scheme I. When followed by $Re^{II} \leftarrow Re^I$ electron transfer across the bridge, eq 4, a slightly higher energy (0.1 eV) mixed-valence isomer is formed.[31] In this

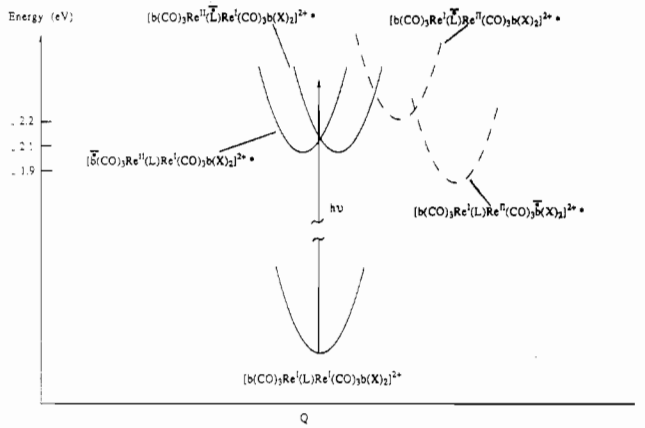


**Figure 10.** Schematic potential energy curves for an averaged librational mode of the solvent, illustrating the flow of electron-transfer events in mechanism 2. The libration is assumed to be a harmonic oscillator that responds to the changes in electronic configuration accompanying each electron-transfer step. The abbreviations used are b for bpy, $b(X)_2$ for $b(CO_2Et)_2$, and L for 4,4'-bipyridine. The dashed curves portray those states that are not accessible by direct excitation of $Re^I$(bpy).

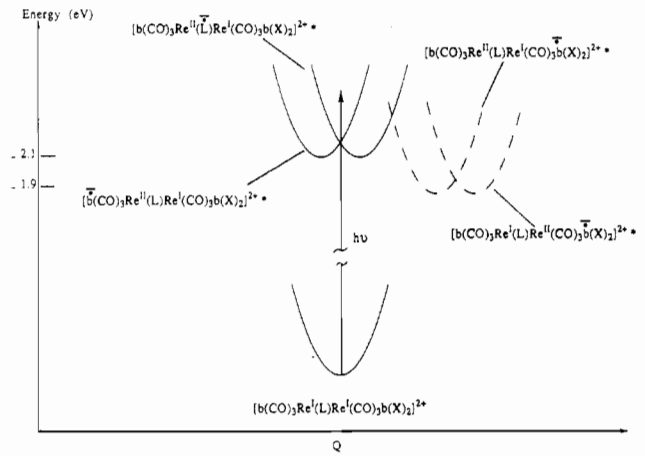


**Figure 11.** Schematic potential energy curves as in Figure 10 but for mechanism 3.

(28) (a) Sullivan, P. D.; Fong, J. Y. *Chem. Phys. Lett.* **1976**, *38*, 555. (b) Kirin, D. *J. Phys. Chem.* **1988**, *92*, 3691. (c) Swiatkowski, G.; Menzel, R.; Rapp, W. *J. Lumin.* **1987**, *37*, 183. (d) Eaton, V. J.; Steel, D. *J. Chem. Soc., Faraday Trans. 2* **1973**, 1601. (e) Carreira, L. A.; Towns, T. G. *J. Mol. Struct.* **1977**, *41*, 1.

(29) (a) Levine, I. R. *Quantum Chemistry*; Allen and Bacon: Boston, MA, 1983. (b) Parr, R. G.; Crawford, B. L., Jr. *J. Chem. Phys.* **1948**, *16*, 526. (c) Dewar, M. J. *J. Am. Chem. Soc.* **1952**, *74*, 3345.

(30) (a) Stephens, F. S.; Vagg, P. S. *Inorg. Chim. Acta* **1982**, *42*, 139. (b) Bukowska-Stryzewska, M.; Tosik, A. *Acta Crystallogr., Sect. B* **1982**, *B38*, 265, 950.

$$[(b)(CO)_3Re^{II}(4,4'\text{-}bpy^{\bullet-})Re^{I}(CO)_3(b(CO_2Et)_2)]^{2+*} \rightarrow [(b)(CO)_3Re^{I}(4,4'\text{-}bpy^{\bullet-})Re^{II}(CO)_3(b(CO_2Et)_2)]^{2+*} \quad (4)$$

mechanism, the overall energy-transfer process is completed by 4,4′-bpy$^{\bullet-}$ → b(CO$_2$Et)$_2$ electron transfer, eq 5. This reaction is favored by 0.25 eV. The excited states involved in mechanism

$$[(b)(CO)_3Re^{I}(4,4'\text{-}bpy^{\bullet-})Re^{II}(CO)_3(b(CO_2Et)_2)]^{2+*} \rightarrow [(b)(CO)_3Re^{I}(4,4'\text{-}bpy)Re^{II}(CO)_3(b^{\bullet-}(CO_2Et)_2)]^{2+*} \quad (5)$$

2 and their relative energies are illustrated in Figure 10. The potential energy curves for the averaged librational modes of the surrounding solvent shown in Figures 10 and 11 are only schematic. Neither their relative positions along the coordinate axis nor the implied force constants are known. One nuance that emerges from this excited-state analysis is the existence of *two* 4,4′-bpy-based MLCT states. This is a situation inherent in systems like these where the sites across the ligand bridge are chemically unsymmetrical. In this case the second bridge-based state, (4,4′-bpy$^{\bullet-}$)Re$^{II}$(b(CO$_2$Et)$_2$), is at a higher energy by ~0.2 eV, which creates a barrier to electron-transfer-induced energy transfer across the bridge.

**Mechanism 3.** In the second electron-transfer mechanism, the initial step from the bridge-based state is by 4,4′-bpy$^{\bullet-}$ → b(CO$_2$Et)$_2$ electron transfer, reaction 6, for which $\Delta G \sim -0.25$ eV.[32]

$$[(b)(CO)_3Re^{II}(4,4'\text{-}bpy^{\bullet-})Re^{I}(CO)_3(b(CO_2Et)_2)]^{2+*} \rightarrow [(b)(CO)_3Re^{II}(4,4'\text{-}bpy)Re^{I}(CO)_3(b^{\bullet-}(CO_2Et)_2)]^{2+*} \quad (6)$$

This creates a "remote" MLCT state in which the photoproduced reductive and oxidative equivalents are separated by ~11 Å across the ligand bridge, Figure 11.[6]

The remote state is the third of three mixed-valence isomers, $[(b^{\bullet-}(CO)_3)Re^{II}(4,4'\text{-}bpy)Re^{I}(CO)_3(b(CO_2Et)_2)]^{2+*}$, $[(b)(CO)_3Re^{II}(4,4'\text{-}bpy^{\bullet-})Re^{I}(CO)_3(b(CO_2Et)_2)]^{2+*}$, and $[(b)(CO)_3Re^{II}(4,4'\text{-}bpy)Re^{I}(CO)_3(b^{\bullet-}(CO_2Et)_2)]^{2+*}$, which differ in the choice of bpy, 4,4′-bpy or b(CO$_2$Et)$_2$ as the electron acceptor ligand. There are three additional isomers based on the same acceptor ligands and the oxidation state distribution Re$^{I}$–Re$^{II}$. The remote MLCT excited state is not accessible by direct excitation to any significant degree because of the absence of significant electronic coupling between the Re$^{I}$ donor and b(CO$_2$Et)$_2$ acceptor.

In mechanism 3, the overall energy transfer is finally achieved by intramolecular Re$^{II}$ ← Re$^{I}$ electron transfer, reaction 7. The

$$[(b)(CO)_3Re^{II}(4,4'\text{-}bpy)Re^{I}(CO)_3(b^{\bullet-}(CO_2Et)_2)]^{2+*} \rightarrow [(b)(CO)_3(CO)_3Re^{I}(4,4'\text{-}bpy)Re^{II}(CO)_3(b^{\bullet-}(CO_2Et)_2)]^{2+*} \quad (7)$$

series of excited states involved in mechanism 3 is illustrated in Figure 11.

Our estimates suggest that the energies of the final $[(b)(CO)_3Re^{I}(4,4'\text{-}bpy)Re^{II}(CO)_3(b^{\bullet-}(CO_2Et)_2)]^{2+*}$ and remote MLCT excited states $[(b)(CO)_3Re^{II}(4,4'\text{-}bpy)Re^{I}(CO)_3(b^{\bullet-}(CO_2Et)_2]^{2+*}$ are comparable. The transient absorbance difference spectrum of the complex shows that $[(b)(CO)_3Re^{I}(4,4'\text{-}bpy)Re^{II}(CO)_3(b^{\bullet-}(CO_2Et)_2)]^{2+*}$ is the dominant form. This conclusion is based on the appearance of the narrow absorption feature at 385 nm. It appears at the same energy as the maximum in the spectrum of $[(b^{\bullet-}(CO_2Et)_2)(CO)_3Re^{II}(4\text{-}Etpy)]^{+*}$. For excited states in which the excited electron is localized in a bpy ligand adjacent to the Re$^{I}$, as it is in the remote MLCT excited state, the absorption in the ($b^{\bullet-}$) $\pi \rightarrow \pi^*$ region is much broader and less well-defined.[33]

**Acknowledgments** are made to P. Chen for the preparation of the 4-Etpy complexes, to the National Science Foundation under Grant CHE-8806664 for support of this research, and to RHONE-POULENC GROUP for support for G.T.

(31) The estimated energy of this state was based on the electrochemical results in Table I and the difference in potential between the Re(II/I) couples in $[(b)(CO)_3Re^{I}(4,4'\text{-}bpy)Re^{I}(CO)_3(b(CO_2Et)_2)]^{2+}$. The assumption was made in this estimate that the difference between Re(II/I) couples is the same regardless of whether the bridging ligand is, 4,4′-bpy or 4,4′-bpy$^{\bullet-}$.

(32) The energy of the remote MLCT excited state was estimated as the difference in potentials between the 4,4′-bpy$^{0/-}$ and b(CO$_2$Et)$_2^{0/-}$ couples in $[(b)(CO)_3Re^{I}(4,4'\text{-}bpy)Re^{I}(CO)_3(b(CO_2Et)_2)]^{2+}$.

(33) (a) Duesing, R. Unpublished results. (b) Chen, P.; Danielson, E.; Meyer, T. J. *J. Phys. Chem.* **1988**, *92*, 3708.